HHS Public Access

Author manuscript

J Comp Physiol B. Author manuscript; available in PMC 2019 November 01.

Published in final edited form as:

J Comp Physiol B. 2018 November ; 188(6): 899–918. doi:10.1007/s00360-018-1164-3.

Mammalian urine concentration: a review of renal medullary architecture and membrane transporters

C. Michele Nawata[1,*] and **Thomas L. Pannabecker**[1]

[1]Department of Physiology, Banner University Medical Center, University of Arizona, 1501 N. Campbell Avenue, Tucson, AZ, USA 85724-5051

Abstract

Mammalian kidneys play an essential role in balancing internal water and salt concentrations. When water needs to be conserved, the renal medulla produces concentrated urine. Central to this process of urine concentration is an osmotic gradient that increases from the corticomedullary boundary to the inner medullary tip. How this gradient is generated and maintained has been the subject of study since the 1940's. While it is generally accepted that the outer medulla contributes to the gradient by means of an active process involving countercurrent multiplication, the source of the gradient in the inner medulla is unclear. The last two decades have witnessed advances in our understanding of the urine-concentrating mechanism. Details of medullary architecture and permeability properties of the tubules and vessels suggest that the functional and anatomic relationships of these structures may contribute to the osmotic gradient necessary to concentrate urine. Additionally, we are learning more about the membrane transporters involved and their regulatory mechanisms. The role of medullary architecture and membrane transporters in the mammalian urine-concentrating mechanism are the focus of this review.

Keywords

kidney; urea transporters; aquaporins; renal medulla

INTRODUCTION

Maintaining water homeostasis, balancing water intake with loss, is essential for health maintenance and life. Mammalian kidneys can adjust the concentration of urine in response to hydration status; conserving water by concentrating the urine when the body is dehydrated and diluting the urine when water is in excess. Water excretion is regulated independently from solute excretion thereby allowing urine osmolality to vary while blood osmolality remains near constant (Jamison and Gehrig 2011).

The ability to concentrate urine varies across species with urine osmolality in humans ranging from 20 - 1200 mOsm kg^{-1} H_2O (Jamison and Gehrig 2011) and exceeding 9000 mOsm kg^{-1} H_2O in the Australian hopping mouse (Beuchat 1996). Although water availability is a main factor influencing urine concentration, anatomical differences between

*Author for correspondence: cmnawata@gmail.com, Telephone: 403-998-9829.

species (Bankir and Rouffignac 1985), metabolic rate (Aw et al. 2018; Beuchat 1996), protein content in diet (Bankir and Kriz 1995), and gender (Perucca et al. 2007) may also have a role.

The kidneys maintain an axial osmotic gradient from the corticomedullary boundary to the inner medullary tip. The cortical tissue is isotonic to the plasma and that of the inner medullary tip is hypertonic to the plasma (Knepper 1982). This gradient, formed mainly by NaCl and urea, becomes steeper during antidiuresis and decreases in magnitude during diuresis (Jamison and Gehrig 2011).

The renal medulla is the main site of urinary concentration and dilution where the vasa recta, loops of Henle, and the collecting ducts (CDs) participate in the countercurrent and co-current exchange of water and solutes (Lemley and Kriz 1987). In the outer medulla (OM), the osmotic gradient is generated by the active reabsorption of NaCl from the thick ascending limbs (TALs) of Henle's loop (Burg 1982). The source of the gradient in the inner medulla (IM) is unknown and although controversial, may involve the passive diffusion of NaCl into the inner medullary interstitium from the ascending thin limbs of Henle's loop (ATLs) (Kokko and Rector 1972; Stephensen 1972) (Fig.1).

Medullary blood flow and hormone regulation have important roles in the urine-concentrating mechanism. The countercurrent exchange of water and solutes between the ascending vasa recta (AVR) and descending vasa recta (DVR) and the interstitium preserves the osmotic gradient by preventing the rapid transfer of solutes away from the medulla (Pallone et al. 2012). Decreased medullary blood flow increases urine osmolality and may be regulated by the vasoconstrictive actions of the antidiuretic hormone arginine vasopressin (AVP) (Francini and Cowley 1996). AVP acts on several mammalian nephron sites (Skorecki et al. 2011) but it exerts its greatest effect on the CDs to reduce urinary water excretion by increasing water permeability and expediting water reabsorption from the CDs back into the circulation (Jamison and Gehrig 2011).

Early studies of inner medullary structure (Kriz 1981; Lemley and Kriz 1967) and more recent three-dimensional reconstructions of the IM (Dantzler et al. 2014; Pannabecker et al. 2008a) suggest that the arrangement of tubular and vascular structures are important for urine concentration. These later studies used mathematical modeling to reveal how the permeability properties of nephron segments and their three-dimensional arrangements may contribute to urine concentration in the IM (Layton et al. 2004; Pannabecker et al. 2008a).

Urea plays an essential role in urine concentration (Gamble et al.1934; Sands and Layton 2014; Yang and Bankir 2005) and specific transporters for urea have been characterized (Sands and Blount 2014). Water transport via aquaporins (AQPs) (Nielsen et al. 2002) and sodium transport via the Na^+-K^+-$2Cl^-$ cotransporter 2 (NKCC2) in the TALs (Ares et al. 2011; Mount 2014) also contribute to the urine-concentrating mechanism.

In this review, we briefly summarize the main concepts underlying the mammalian urine-concentrating mechanism. More comprehensive discussions can be found elsewhere (e.g. Pannabecker 2013; Sands and Layton, 2014). We then focus on renal medullary architecture

and membrane transporters that contribute to the urine-concentrating mechanism, highlighting recent developments.

ROLE OF THE OUTER MEDULLA

Countercurrent multiplication

The generally accepted model of the urine-concentrating mechanism first proposed by Kuhn and Ryfell (1942) and modified over the years involves countercurrent multiplication. The multiplication of a small osmolality difference between countercurrent flows in the limbs of Henle's loop at each level in the OM establishes a large corticomedullary osmolality gradient (Gottschalk and Mylle 1959). This gradient is maintained by the active reabsorption of NaCl from the TALs into the interstitium which raises the interstitial osmolality and promotes the reabsorption of water from the thin descending limbs of Henle's loop (DTLs) and CDs (Burg 1982; Gottschalk and Mylle 1959; Lassiter et al. 1961).

Alternatives to countercurrent multiplication

The countercurrent multiplication model assumes that the opposing flows in the loops are in proximity to one another. However, the DTLs of short-looped nephrons are located close to or within vascular bundles and are therefore separated anatomically from the TALs (Kriz 1981). Additionally, since the water channel AQP1 is not (or is weakly) expressed in the lower portion of the DTLs in the short-looped nephrons (Nielsen et al. 1995; Wade et al. 2000; Zhai et al. 2007) the contribution of these sections to water reabsorption is questionable. An alternative to the countercurrent multiplication model involves active NaCl reabsorption without accompanying water reabsorption from the short-looped DTLs (Layton and Layton 2011). In this model, the osmolality gradient is sustained by an increasing ratio of NaCl relative to water as a function of depth in the OM. Most water is absorbed in the upper OM from the long-looped DTLs and CDs and therefore the water load in the deep OM is low. Higher Na^+-K^+-ATPase activity in the deep OM promotes greater NaCl reabsorption from the TALs (Layton and Layton 2011).

Kangaroo rats have the ability to produce urine that is more concentrated than the maximum concentrated urine of common laboratory rats (6000 mOsmol kg^{-1} H_2O vs. 3000 mOsmol kg^{-1} H_2O; Beuchat 1996). Aw et al. (2018) reported that outer medullary Na^+-K^+-ATPase is higher at the activity, protein, and mRNA levels in the kangaroo rat than in Munich-Wistar and Sprague-Dawley rats. Thus, higher Na^+-K^+-ATPase activity may be a contributing factor to a steeper osmotic gradient and therefore higher maximal urine concentrating ability in kangaroo rats. This also supports the hypothesis that active NaCl transport, rather than countercurrent multiplication is key to the generation of the osmotic gradient in the OM (Layton and Layton 2011).

ROLE OF THE INNER MEDULLA

Passive mechanism

The commonly cited mechanism for urine concentration in the IM is the passive mechanism proposed by Kokko and Rector (1972) and Stephenson (1972). In this model, the continuous

diffusion of urea into the inner medullary interstitium from the inner medullary collecting duct (IMCD) raises the interstitial urea concentration, drawing water from the DTLs and IMCD and consequently reducing the interstitial NaCl concentration. The DTLs with low NaCl and urea permeability continuously deliver fluid high in NaCl to the ATLs so that the ATL fluid has a higher NaCl concentration but lower urea concentration than the interstitium. Under these conditions, NaCl will tend to diffuse out and urea will tend to diffuse into the ATLs (Fig. 1). However, if urea permeability is lower than that of NaCl in the ATL, NaCl efflux will exceed urea influx. The result is a dilution of ATL fluid that flows away from the IM, elevating the interstitial osmolality at each level as it ascends.

Alternatives to the passive mechanism

The passive model has failed to gain general acceptance as inconsistencies exist between measured urea and NaCl permeabilities in the loops of Henle and proposed steady-state models for inner medullary solute concentration (reviewed by Knepper et al. 2003). As a result, several alternative hypotheses have been proposed. Osmotically active particles such as lactate could act as concentrating agents in the IM (Hervy and Thomas 2003; Jen and Stephensen 1994; Thomas 2000) or pelvic wall contractions could serve as an energy source for the concentrating process (Schmidt-Nielsen 1995) with hyaluronan acting as a mechano-osmotic transducer to convert contractions into an osmolality gradient (Knepper et al. 2003). However, these alternatives have not yet been explored further experimentally and the inner medullary concentrating mechanism remains an enigma.

MEDULLARY FUNCTIONAL ARCHITECTURE

Architecture and tubular fluid flows

Tubule functional heterogeneity plays an important role in the process of solute recycling between nephron segments, vasa recta and the interstitium and production of the corticomedullary solute gradient. Nephron and blood vessel segments, which exhibit solute-specific epithelial transport pathways, are juxtaposed in a highly organized fashion throughout the medulla. The discrete juxtapositions of these nephrons and vessels underlie specific solute exchange, cycling and sequestration processes that are related to the urine-concentrating mechanism and medullary and renal function more generally (Chen et al. 2009a,b, 2010; Fry et al. 2014; Knepper and Roch-Ramel 1987; Layton et al. 2010; Layton 2011; Lemley and Kriz 1987; Pannabecker and Layton 2014; Pannabecker et al. 2008a; Thomas and Wexler 1995; Wang et al. 1998). Therefore, a detailed understanding of the renal functional architecture is needed for developing a more complete understanding of the preferential fluid and solute flows that occur between the many tubular and interstitial compartments throughout the medulla to produce the axial solute gradient.

The medulla consists of distinct structurally defined zones that lie along the corticomedullary axis and regions that lie perpendicular to (lateral to) the corticomedullary axis. In most rodents, the OM consists of two zones including the outer stripe of the outer medulla (OSOM) and the inner stripe of the outer medulla (ISOM) (Fig. 2) and two lateral regions including the vascular bundle and the interbundle regions (Fig. 3) (Bankir and De Rouffignac 1985; Lemley and Kriz 1987). Vascular bundles lie within the vascular bundle

regions and are absent from the interbundle regions. The IM, as reported for rat, kangaroo rat and human, also consists of two zones that include an outer zone and an inner zone (also referred to as the upper and lower inner medulla, respectively) (Fig. 2) and two lateral regions that include the intracluster and intercluster regions (Issaian et al. 2012; Pannabecker et al. 2008b; Urity et al. 2012; Wei et al. 2015) (Fig. 3). Clusters of CDs lie within the intracluster regions and are absent from the intercluster regions. The two lateral regions of the ISOM and inner medulla are shown in transverse tissue sections in Fig. 4.

The following two sections summarize the axial zonation and lateral regionalization of the medulla and the tubulovascular morphology that have been studied primarily in the rat, mouse, hamster, chinchilla and kangaroo rat.

Nephron and collecting duct segmentation

In the rat, there are about 7,000 largely unbranched CD segments in the OM, and they gradually coalesce as they descend through the IM (Oliver 1968; Saxen 1987). Approximately 30 CDs at the OM-IM boundary coalesce into approximately 5 primary CD clusters, which then combine into a single CD in the deep papilla to form a single secondary CD cluster. Secondary clusters continue to join together to form approximately 10-15 ducts of Bellini at the papilla tip (Pannabecker and Dantzler 2007). CDs consist of two cell types in the OM, the intercalated and principal cells, at about a 2:3 ratio. Approximately 10% of the CD cells in the initial third of the IM are intercalated, whereas CDs of the terminal two-thirds of the IM consist of a single structurally and functionally distinct cell type, the “IMCD” cell (Christensen et al. 2012; Clapp et al. 1989; Madsen et al. 1988).

Each medullary nephron descends from its originating glomerulus and enters the OSOM as the loop of Henle, which consists of the pars recta of the proximal tubule, the DTL, the ATL (in long-looped nephrons only) and the TAL (Christensen et al. 2012). While the OSOM and its distinctive nephron and vascular architecture have been well-defined in the rodent kidney (Christensen et al. 2014; Lemley and Kriz 1987; Zhai et al. 2006), the architecture of the superficial OM in the human and pig kidney is less clear. Several past observations (Kriz 1981; Peter 1909) and one recent preliminary report (Pannabecker and Rosen 2017) suggest that the human and pig OSOM is minimal or absent altogether. In the latter two species, unlike the rodent, the medullary rays appear to dominate the corticomedullary boundary, fusing with composite groupings of venous vasa recta, CDs and TALs in the superficial OM.

There are two types of medullary nephrons based on morphological criteria: short-looped nephrons and long-looped nephrons. The short-looped nephron forms a 180-degree bend in the OM. In most species, the bends appear at all levels in the OM, with most bends forming near the OM-IM boundary; however, in the human and pig, the bend also forms in the cortex (Kaissling and Kriz 1992). By contrast, the long-looped nephrons form their bend in the IM, also at all levels in most species. As a consequence, the total nephron number at each transverse level gradually declines with depth below the cortex.

In the mouse, three types of bends have been identified in the short-looped nephron, with the junction between the DTL and the TAL of the short-looped nephron occurring prior to,

within or following the bend (Zhai et al. 2006). TALs of short-looped and long-looped nephrons lie in the OM and medullary rays and labyrinth of the cortex.

The thin limbs of Henle's loops are structurally and functionally heterogeneous (Chou and Knepper 1992, 1993; Nawata et al. 2014), with the short-looped DTL consisting of the type 1 epithelium. The long-looped DTL consists sequentially of the type 2 and 3 epithelia, and a short prebend segment and the ATL consist of the type 4 epithelium (Bachmann and Kriz 1982; Chou et al. 1993; Jamison and Kriz 1982; Kaissling and Kriz 1992; Kriz 1981; Schwartz et al. 1979; Schwartz and Venkatachalam 1974; Zhai et al. 2006). The ATL abruptly transitions into the TAL of the ISOM. TALs of the inner stripe are morphologically distinct from those of the OSOM and cortex, exhibiting greater cell height, more abundant mitochondria, and deeper and more extensive and complex invaginations of the basal plasmalemma (Kone et al. 1984).

Water reabsorption by the long-looped DTLs plays an important role in osmotic equilibration between the luminal fluid and the interstitium, and equilibration is considered to be required in the urine-concentrating mechanism. In the mouse, significant convolutions in the outer part of the ISOM increase the length of this segment by approximately 27%, potentially contributing to effective fluid reabsorption and a high urine concentrating ability in this species (Zhai et al. 2006). There is little or no expression of the water channel AQP1 in the short-looped DTL of the rat and mouse (Wei and Pannabecker, unpublished; Zhai et al. 2007), and in the absence of expression of other AQPs in the descending thin limbs, it seems unlikely that water channels play a significant role in water reabsorption in the short-looped DTLs. One published study reported a significant water permeability in these segments in the hamster; however, this study has not been replicated and the authors reported difficulty in distinguishing between segment types 1 and 2 in vitro (Imai et al. 1984). It has been shown in the rat and kangaroo rat IM that AQP1 is expressed along only approximately 40% of the length of the inner medullary portion of the long-looped DTL. In other words, the expression of AQP1 along the length of the long loop DTL is proportional to the depth at which that segment forms its bend (Pannabecker and Dantzler 2004, 2008; Urity et al. 2012). For most long-looped DTLs, AQP1 is expressed continuously through the OM; however, for those DTLs that form a bend within the first millimeter below the OM-IM boundary, AQP1 is expressed along partial lengths of the outer medullary segments, and there is no detectable expression in the inner medullary segments.

The inner medullary DTL segments that express AQP1 are positioned in the intercluster region (Fig. 3). As each thin limb descends through the IM, it gradually approaches a neighboring CD cluster region, and the terminal portion of its AQP1-negative segment continues its descent within the intracluster region before forming a 180-degree bend, also within the intracluster region (Westrick et al. 2013). Distal to the bend, the ascending segment then rises towards the OM-IM border and gradually moves into the intercluster region at approximately the same level at which its descending segment entered the cluster region.

Vasa recta segmentation

The OM of rats, mice and other rodents is characterized by vascular bundles that are more complex than the simple type found in the rabbit, pig, human and other mammals (Bankir and De Rouffignac 1985; Kriz 1981). The “complex” and “simple” type of medulla, as represented in these species, correlates with high and low urine-concentrating ability, respectively. In mammals that have the simple type of medulla (e.g., rabbits, pigs, and humans) (Bankir and De Rouffignac 1985; Pannabecker 2013), the short-looped DTLs lie within the interbundle region alongside long-looped DTLs, CDs, TALs and branching AVR networks. However, in rodents (e.g., rats, mice and kangaroo rats), which have the complex type of medulla, the short-looped DTLs may be closely associated within or immediately adjacent to the vascular bundles.

The outer medullary vascular bundles consist of DVR (the arterial segments), which arise from efferent arterioles of juxtamedullary glomeruli, and AVR (the venous segments). Within the bundles, both vessel types exhibit little or no branching. DVR terminate at variable depths in their descent along the corticomedullary axis, at which point they connect to a capillary that joins an interbundle network of branching (venous) AVR (Moffat and Fourman 1963; Pallone et al. 2003; Rollhauser et al. 1964). In the rat, the venous capillary networks in the OSOM and the outer part of the ISOM ascend within the interbundle region to join the intrarenal veins at the corticomedullary boundary; whereas, at least some of the venous capillary networks in the inner part of the ISOM join the AVR within the vascular bundles before joining the intrarenal veins (Kriz 1982; Yamamoto et al. 1984). The existence of separate capillary flows in the networks of the OSOM and the ISOM would imply that a degree of functional independence may exist between the OSOM and the ISOM in the rat. By contrast, in the mouse, no connections were observed between the capillaries of the interbundle networks and the AVR within the bundles in three-dimensional reconstructions along the entire corticomedullary axis of the OM (Ren et al. 2014).

No differences in the cellular structure of non-branching and branching AVR have been identified. While fluid and solute permeabilities have never been experimentally quantified in non-branching and branching AVR, both types are covered with plaques of fenestrae and are considered to have very high permeability to water and small solutes (MacPhee and Michel 1995; Michel and Curry 1999; Pallone et al. 1994, 2003).

In the IM, the intercluster regions include a vascular bundle consisting of non-branching vessels. The intracluster regions include networks of branching AVR that are relatively sparse compared to the capillary networks of the ISOM. The inner medullary DVR connect to capillaries that join the intracluster AVR networks at variable depths along the corticopapillary axis. DVR that extend into the deep papilla enter into a zone consisting primarily of branching AVR, some of which ascend through the vascular bundles as non-branching AVR. Offshoots of AVR within the intracluster capillary networks connect to AVR within a vascular bundle along the corticomedullary axis of the IM (Kim and Pannabecker 2010; Kriz 1982; Yuan and Pannabecker 2010).

Branching AVR and CDs are closely juxtaposed within the intracluster region, and they maintain this close abutment with each other throughout the entire inner medulla forming

microdomains of interstitial space known as “interstitial nodal spaces” (Pannabecker and Dantzler 2006). Interstitial nodal spaces are bounded by a single CD, two AVR and one or two ATLs that lie opposite the CD (Fig. 5). This arrangement gives rise to distinct countercurrent flows, with the CDs carrying fluid and solutes toward the tip of the papilla, and the AVR and ATLs carrying fluid and solutes in a cortical direction. Interstitial nodal spaces may be capped by interstitial cells that lie approximately 1-10 μm apart along the corticomedullary axis (Lemley and Kriz 1991) to form stacks of interstitial nodal space compartments. It has been proposed that these compartments serve as chambers for localized mixing of urea from the CDs and NaCl from the ATLs in support of the urine-concentrating mechanism (Layton et al. 2009, 2012).

TRANSPORTERS

Aquaporins (AQPs)

Thirteen mammalian AQP isoforms have been identified so far with at least nine of these expressed in the kidney (Michalek 2016). AQP 1, 2, 3, and 4 are the most studied in the kidney and based on knockout studies, AQP 1, 2, and 3 are essential for urine concentration (Fenton and Knepper, 2007; Nielsen et al. 2002).

AQP 2, 3, and 4 can be regulated acutely and chronically by phosphorylation events stimulated by AVP. When AVP binds to its receptors (V2R) in the basolateral membrane of CDs, intracellular cAMP levels are increased, protein kinase A (PKA) is activated, and phosphorylation takes place (Boone and Deen 2008). Acute increases in AVP promote the translocation of AQP2-containing vesicles to the apical plasma membrane (Nielsen et al. 2002). Chronically elevated levels of circulating AVP, water deprivation, and desmopressin (dDAVP) administration have been shown to increase the abundance of AQP2 and AQP3 (Nielsen et al. 1993; Terris et al. 1996) and AQP4 (Poulsen et al. 2013; van Hoek et al. 2009). The regulation of AQPs by AVP has been well-documented and several reviews are available (e.g. Boone and Deen 2008; Jung and Kwon 2016; Nielsen et al. 2002).

AQP1—AQP1 contributes to constitutive water permeability and is expressed in the apical and basolateral plasma membranes of the proximal tubule, DTLs, and DVR (Nielsen et al. 1995; Zhai et al. 2007) (Fig. 6). The axial heterogeneity of AQP1 expression in DTL segments (Nielsen et al. 1995; Wade et al. 2000; Zhai et al. 2007) closely parallels the water permeability characteristics of these sections (Chou and Knepper 1992, 1993; Chou et al. 1993; Nawata et al. 2014). Humans lacking functional *AQP1* (King et al. 2001) and *AQP1* knockout mice (Ma et al. 1998) have impaired urine concentrating ability.

AQP2—AQP2 is expressed in the apical and basolateral plasma membranes as well as in subapical vesicles in the CDs (Nielsen et al. 1993) (Fig. 6, 7). CD segments are nearly impermeable to water in the absence of AVP, except the terminal IMCD which has moderate water permeability in the absence of AVP (Sands et al. 1987). Mutations in the *AQP2* gene cause nephrogenic diabetes insipidus in humans (Rutishauser and Kopp 1999), and rats with lithium-induced diabetes have reduced AQP2 expression (Marples et al. 1995). Rats and mice with streptozotocin (STZ)-induced diabetes have increased AQP2 expression (e.g. Bardoux et al. 2001; Satake et al. 2010) which is thought to be a compensatory mechanism

to alleviate dehydration due to polyuria (Nejsum et al. 2001; Kim et al. 2003; Satake et al. 2010).

AQP3—AQP3 is expressed in the basolateral membranes of the CDs in the cortex, OM, and IM (Fig. 6, 7) with highest expression in the base of the IM (Ecelbarger et al. 1995; Frigeri et al. 1995; Ishibashi et al. 1994; Ma et al. 1994). The importance of AQP3 for urine concentration is demonstrated in *AQP3* knockout mice that exhibit impaired urine concentration with severe polyuria (Ma et al. 2000). However, these knockouts also have decreased AQP2 in the cortex which may contribute to the polyuria (Nielsen et al., 2002). AQP3 protein expression increases when rats are dehydrated for two days (Ecelbarger et al. 1995; Terris et al. 1996). AQP3 also increases in rats unable to produce AVP (Brattleboro rats) after they are infused with AVP for five days (Terris et al. 1996).

AQP4—AQP4 co-localizes with AQP3 in the basolateral membrane of the IMCD (Fig. 6, 7), with strongest expression near the base of the IM and weaker expression in the tip of the IM (Frigeri et al. 1995; Terris et al. 1995). *AQP3/AQP4* double knockouts have a much greater urine concentrating defect than single *AQP3* knockouts (Ma et al. 2000), and *AQP4* knockouts have only a mild concentrating defect (Chou et al. 1998; Ma et al. 1997). Isolated IMCDs from *AQP4*-null mice display a four-fold reduction in AVP-stimulated water permeability (Chou et al. 1998). Thus, AQP4 may be responsible for the majority of the AVP-stimulated basolateral water movement in the IMCD, whereas AQP3 may have a greater role in the more proximal regions of the CD (Nielsen et al. 2002). Terris et al. (1996) reported that AQP4 expression in Sprague-Dawley rats was unresponsive to water restriction, and 5-day AVP administration in Brattleboro rats did not change AQP4 expression. However, van Hoek et al. (2009) showed that 8-day administration of dDAVP to Brattleboro rats increased AQP4 expression. In another study, 6-day infusion of dDAVP in Brattleboro rats increased the AQP4 protein abundance in first third of the IMCD (IMCD1) and decreased in the remaining two thirds of the IMCD (IMCD2 and IMCD3) (Poulsen et al. 2013).

Regulators of AQP2

In their review, Olesen and Fenton (2017) discuss the recent concept that V2R-mediated AQP2 membrane targeting is not dependent on cAMP and that other mechanisms may be involved. Indeed, there are many mediators or hormones that regulate AQP2 and they can act either dependently or independently of AVP and the cAMP-PKA pathway. In vitro and in vivo studies have shown that hyperosmolality increases AQP2 abundance independent of AVP stimulation (Hasler et al. 2009) and tonicity response element-binding protein is likely involved (Hasler et al. 2009; Lam et al. 2004). The hormones of the renin-angiotensin-aldosterone system, angiotensin II (Lee et al. 2007) and aldosterone (Hasler et al. 2009) have been reported to regulate AQP2. Other AQP2 regulators include oxytocin and secretin (Bai et al. 2017), integrin-linked kinase (Cano-Penavler et al. 2014), insulin, nuclear factor, fluid shear stress, extracellular pH, glycogen synthase kinase 3, 14-3-3 proteins, and phosphatases (reviewed by Hasler et al. 2009; Jung and Kwon 2017). Inhibitors of AQP2 include bradykinin, nitric oxide, adenosine, ATP, and endothelin (reviewed by Olesen and Fenton,

2017; Pearce et al. 2015). Some other recent findings involving AVP-dependent and AVP-independent control of AQP2 are described in the following section.

AVP-dependent control of AQP2

PGE_2, EP3, EP4, PRR—The lipid mediator prostaglandin E2 (PGE_2) has four G-protein coupled receptors (EP1-4) throughout the nephron segments (Li et al. 2017). PGE_2 or sulprostone (an agonist for EP1 and EP3) decreases AVP-induced water reabsorption and AQP2 membrane targeting, while EP2 and EP4 are associated with increased AQP2 abundance (Olesen et al. 2011, 2016). A study by Hassouneh et al. (2016) reported that in STZ mice, EP3 is upregulated and cortical and medullary AQP2 is decreased. The discrepancy between this finding and previous reports (e.g. Bardoux et al. 2001) that demonstrated increased AQP2 in STZ mice may be due to differences in species, stage, or strain used in the studies (Hassouneh et al. 2016). When EP3 is deleted in STZ mice, AQP2 expression increases, and therefore EP3 may be responsible for renal resistance to AVP (Hassouneh et al. 2016). EP4 appears to have a role in AQP2 membrane targeting and abundance. In the medullary tissue of water-deprived mice, EP4 is increased and *EP4* knockouts have impaired urine concentration with decreased AQP2 expression and membrane targeting (Li et al. 2017).

Prorenin receptor (PRR), a component of renin-angiotensin-aldosterone system, regulates prorenin and renin catalytic activity (Nguyen et al. 2002) and is expressed in the intercalated cells of the CD (Advani et al. 2009). *PRR* knockout mice have decreased urine osmolality, increased urine volume, and reduced medullary AQP2 protein (Ramkumar et al. 2015; Wang et al. 2016a). Water restriction increases the PPR protein levels in rat kidneys (Tamura et al. 2016; Wang et al. 2016a) and water-restricted rats infused with an inhibitor that interrupts the binding of prorenin to PRR, have reduced AQP2 expression (Wang et al. 2016a). Based on studies in IMCD cells, Wang et al. (2016a) proposed a linear pathway for AQP2 regulation and expression in the water-restricted rat (AVP→PGE_2→EP4→PRR). AVP stimulates PGE_2 release that sequentially activates the EP4 receptor and PRR; PRR then stimulates an increase in AQP2 expression which enhances urine concentration.

Soluble prorenin receptor (sPRR) is produced by the intracellular cleavage of PRR (Cousin et al. 2009) and is increased in the urine (Wang et al. 2016a) and plasma (Tamura et al. 2006) of water-restricted rats. The biological role of sPRR is unknown, but Lu et al. (2016) found that sPRR increased AQP2 protein in rat IMCD cells and this process relied on frizzled-8-dependent -catenin signaling and cAMP-PKA pathways.

FXYD1—FXYD proteins are a family of small membrane proteins that regulate the transport properties of Na^+-K^+-ATPase, and several FXYD members are present in the kidney (Geering 2006). FXYD1 is expressed in the IMCDs of mice and dDAVP treatment induces dephosphorylation of FXYD1 and translocation of FXYD1 and AQP2 to the apical plasma membrane (Arystarkhova et al. 2017). *FXYD1* knockout results in dilute daytime urine with lower AQP2 abundance in the IM and reduced AQP2 retention in the apical membrane. Therefore, the role of FXYD1 may be to enhance AQP2 retention in the apical membrane of the IMCD (Arystarkhova et al. 2017).

Purinergic $P2Y_{12}$ receptor ($P2Y_{12}$-R)—$P2Y_{12}$-R, a G-protein coupled purinergic receptor found mostly on platelets, functions as a chemoreceptor for ADP and reduces cAMP levels (Dorsam and Kunapuli 2004). $P2Y_{12}$-R is also present in the rat kidney and inhibition of this receptor results in increased urine concentration and AQP2 protein in Sprague-Dawley rats but not in Brattleboro rats (Zhang et al. 2015). Furthermore, blocking $P2Y_{12}$-R in primary rat IMCD cells treated with dDAVP potentiates the expression of AQP2 and AQP3 and increases cAMP production (Zhang et al. 2015).

AVP-independent control of AQP2

Micro RNA—Micro RNA (miRNA) are small non-coding RNA molecules that modulate post transcriptional regulation of gene expression by inhibiting translation of target mRNA (Bartel 2004). Luo et al. (2014) showed that miR-466a-3p and related miRNAs were down-regulated by dDAVP in murine IMCD3 cells and transgenic overexpression of miR-466a-3p led to a downregulation of *AQP2* and other osmoregulation-associated genes in the mouse cortex and medulla. Later, Kim et al. (2015) identified two miRNAs (miR-32 and miR-137) that attenuated dDAVP-induced *AQP2* expression in mouse collecting duct ($mpkCCD_{c14}$) cells. AQP2 translation was also decreased in these cells when transfected with miR-32 and miR-137 mimics (Kim et al. 2015).

Nuclear receptors—Nuclear receptors are ligand-activated nuclear transcription factors that regulate gene transcription and expression by binding to hormone response elements in the promoter regions of genes (Sever and Glass 2013). Liver X receptor (LXR) is involved in lipid homeostasis, however it has been reported to regulate renal transporters (Soodvilai et al. 2012). Lu et al. (2016) reported that activation of LXR in mice induced polyuria and reduced expression of AQP2 and PRR, an effect that was reversed with a PRR agonist. LXR exists as and isoforms and therefore this reduction of AQP2 may be due to LXR since LXR activation increases the abundance of AQP2 protein (Su et al. 2017). Other nuclear receptors implicated in water regulation via AQP2 in the CDs include peroxisome proliferator-activated receptor gamma, glucocorticoid receptor, mineralocorticoid or aldosterone receptor, farnesoid X receptor, and estrogen receptor alpha (reviewed by Zhang et al. 2016).

Phosphorylation—Although AVP is the main stimulator of AQP2 phosphorylation, other mechanisms have been described. Recently it was reported that adenosine monophosphate kinase (AMPK) activated by the antidiabetic drug metformin can phosphorylate AQP2 and increase its expression and membrane accumulation in rat IMCDs (Klein et al. 2016a). However, Al-bataineh et al. (2016) demonstrated that AMPK does not significantly phosphorylate AQP2 directly, suggesting that the AMPK effect is likely indirect and mediated by other kinases or phosphatases.

Ubiquitin ligases (E3 ligases)—Another factor that influences the abundance of AQP2 is degradation via the ubiquitin pathway (Jung and Kwon 2016). E3 ligases are responsible for catalyzing the ligation of ubiquitin to its substrate (Dikic and Robertson 2012). In their study, Wu et al. (2018) found that E3 ligase CHIP could directly ubiquitinate AQP2 in vitro, and deletion of CHIP in mice resulted in increased AQP2 abundance, decreased urine volume, and increased urine osmolality. Centrone et al. (2017) reported that CHIP

overexpressed in mouse CD cells increases AQP2 degradation and heat shock protein 70 abundance. The authors hypothesize that heat shock protein 70 tethers to the E3 ligase MDM2 which is directly involved in the ubiquitination and proteasomal degradation of AQP2, while CHIP acts as a chaperone for AQP2 and anchoring protein for MDM2. In another study, Trimpert et al. (2017) showed that knockdown of the E3 ligases *NEDD4* and *NEDD4L* in mpkCCD cells increased AQP2 abundance. They concluded that NEDD4 and NEDD4L mediate the ubiquitination and degradation of AQP2 via the NEDD4 family interacting proteins 1 and 2 which directly interact with AQP2.

Urea Transporters

There are two families of urea transporters; *UT-A* (*Slc14A2*) isolated originally from rabbit IM (You et al. 1993) and *UT-B* (*Slc14A1*) initially cloned from human bone marrow cells (Olives et al. 1994). Isoforms of *UT-A* and *UT-B* are expressed in several mammalian tissues and cell types and several non-mammalian urea transporters have also been identified (Sands and Blount 2014). UT-A1, UT-A2, UT-A3, and UT-B1 are present in the kidney (Sands and Blount 2014). UT-A4 is detected in the rat medulla but in very low abundance and the exact location in the nephron is unknown (Bagnasco et al. 2000; Karakashian et al.1999).

Knockout studies have proven useful for understanding the roles of urea transporters (UTs) in producing concentrated urine (Fenton and Yang 2014; Li et al. 2012). The interest in developing UT inhibitors as diuretics has also stemmed from knockout studies (Klein and Sands 2016). To investigate whether UT inhibitors can be developed into diuretics without serious side effects, Jiang et al. (2017) generated an all-*UT* knockout model. This knockout has a more severe urine concentrating defect than any other single- or double-*UT* knockout (discussed later), but with little abnormality in extrarenal organs.

UTs are subject to both short-term and long-term regulation. Short-term regulation involves factors that alter membrane accumulation of UTs such as phosphorylation, ubiquitination, and glycosylation (Klein 2014). Long-term regulation by water-restriction or AVP (or dDAVP) administration influences the amount of urea transporter available (Klein 2014).

Urea transport is influenced by many other factors including low-protein diet, osmotic diuresis, adrenal steroids, purinergic receptor ($P2Y_2$), electrolyte abnormalities, aging, angiotensin II, 14-3-3 proteins, and sialylation (reviewed by Klein 2014; Klein and Sands 2016).

UT-A1

In the mammalian kidney, UT-A1 is expressed in the apical plasma membrane of the IMCD (Fig. 7) and is phloretin inhibitable (Bagnasco et al. 2001; Nielsen et al. 1996; Shayakul et al. 1996). Because UT-A3 is essentially the amino-terminal half of UT-A1 (Karakashian et al., 1999), it is not possible to create a *UT-A1* knockout without simultaneously knocking out *UT-A3*. *UT-A1/A3* double knockouts exhibit strong urine-concentrating defects with increased urine output and decreased urine osmolality (Fenton et al. 2004). When *UT-A1* is transgenically expressed in *UT-A1/A3* double knockouts, maximal urine concentrating ability is restored (Klein et al. 2016b).

Regulation of UT-A1

Protein kinase A (PKA)—AVP-mediated phosphorylation of UT-A1 leads to the apical plasma membrane accumulation of UT-A1. This occurs through two cAMP-dependent signaling pathways, PKA (Blount et al. 2008) and Epac (exchange protein activated by cAMP) (Wang et al. 2009). PKA phosphorylates UT-A1 at S486 and S499 and at least one of these serines must be phosphorylated to increase urea flux and UT-A1 accumulation in the apical plasma membrane (Blount et al. 2008). Although the site of Epac phosphorylation is unknown, it does not occur at S486 or S499 (Hoban et al. 2015).

Protein kinase C (PKC)—The role of PKC in urine concentration was first reported by Yao et al. (2004) who noted modestly greater urine flow rate and modestly lower urine osmolality in mice lacking *PKC* Subsequent studies have shown that PKC regulates urea permeability in the rat IMCD and this is stimulated by hypertonicity and is independent of AVP (Klein et al. 2012; Wang et al. 2010, 2013).

According to Blount et al. (2015), PKC-mediated phosphorylation of UT-A1 occurs at S494 and activators of cAMP pathways (PKA and Epac) do not increase phosphorylation at this site. They also found that ablating the S494 site decreases UT-A1 abundance in the plasma membrane and activation of the PKC pathway alone does not increase UT-A1 accumulation in the plasma membrane. Indeed, maximal increases in urea transport and increased plasma membrane accumulation of UT-A1 may require stimulation of both cAMP and PKC-signaling pathways (Wang et al. 2010, 2013). The cAMP pathway promotes trafficking to the apical membrane and the PKC phosphorylation pathway results in increased retention in the apical membrane (Blount et al. 2015)

Adenosine monophosphate kinase (AMPK)—AMPK can also phosphorylate UT-A1. When activated by metformin, AMPK phosphorylated UT-A1 in rat IMCDs and increased urea permeability likely by activating UT-A1 already in the membrane and not by increasing apical membrane presence (Klein et al. 2016a).

UT-A2

UT-A2 is expressed in the late part of the short-looped DTLs and in the early inner medullary part of the long-looped DTLs (Shayakul et al. 1997; Wade et al. 2000; Zhai et al. 2007) (Fig. 6). UT-A2 is thought to play a role in intrarenal urea recycling between the DTLs and the ATLs and between the DTLs and the DVR (Wade et al. 2000). Uchida et al. (2005) suggested that the role of UT-A2 may be to maintain high urea when the urea supply to the kidney is limited since *UT-A2* knockouts have only mild urine concentrating defects and only when on a low-protein diet. *UT-A2/UT-B* double knockouts have less severe concentration defects than *UT-B* knockouts indicating that *UT-A2* deletion in these double-knockouts allows urea to accumulate in the IM because urea is not lost to the circulation from the DTLs (Lei et al. 2011). UT-A2 may be involved in the long-term accumulation of urea in the IM since *UT-A2/UT-B* deficient mice were not able to accumulate urea in the IM after an acute urea load (Lei et al. 2011). Fenton and Yang (2014) suggest that UT-A2 contributes to urea accumulation in the IM during the transition from diuresis to antidiuresis rather than maintaining high urea under normal conditions.

Regulation of UT-A2

Urea flux through mouse UT-A2 stably expressed in Madin-Darby canine kidney cells is phloretin inhibitable and acutely increased by AVP, forskolin, and increased intracellular calcium, but PKA may not be involved since the PKA inhibitor H89 has no effect on forskolin-stimulated flux (Potter et al. 2006). UT-A2 protein and mRNA expression increases in the DTLs when rats are water-restricted or dehydrated (Bagnasco et al. 2000; Lim et al. 2006; Nawata et al. 2015; Smith et al. 1995). In Brattleboro rats, dDAVP treatment during dehydration increased *UT-A2* mRNA (Shayakul et al. 2000) and chronic infusion of dDAVP strongly increased UT-A2 protein expression (Wade et al. 2000). In mice, *UT-A2* mRNA increased after fluid restriction, likely resulting from stimulation of the *UT-A* promoter by cAMP (Fenton et al. 2002a).

UT-A3

UT-A3 is expressed in the IMCD (Blount et al. 2007; Lim et al. 2006; Stewart et al. 2004; Terris et al. 2001) (Fig. 6). While transgenic restoration of *UT-A1* in *UT-A1/A3* knockouts revealed a critical role for UT-A1 in urine concentration (Klein et al. 2016b), the role of UT-A3 is less apparent. UT-A3 has been thought to be responsible for basolateral urea transport (Shayakul et al. 2001; Stewart et al. 2007) and has been detected in the basolateral membranes of mice and rat IMCD cells (Lim et al. 2006; Stewart et al. 2004). However, Terris et al. (2001) localized UT-A3 to the apical membrane of rat IMCD cells. Later, Blount et al. (2007) showed that UT-A3 moves to the apical membrane when exposed to AVP and suggested that under basal conditions UT-A3 functions as a basolateral transporter (Fig. 7).

Regulation of UT-A3

UT-A3 is phloretin inhibitable and regulated by cAMP, exhibiting increased urea flux when exposed to forskolin or AVP in heterologous systems (Fenton et al. 2002b; Karakashian et al. 1999; Shayakul et al. 2001; Stewart et al. 2007). The involvement of PKA in UT-A3 phosphorylation is not clear because deletion of the PKA consensus sites in murine UT-A3 does not alter urea transport (Smith et al. 2004) but H89 blocks the AVP stimulation of urea transport through murine UT-A3 (Stewart et al. 2007).

UT-A3 has a single glycosylation site at N279 and mutation of this site reduces forskolin-stimulated membrane expression and urea transport (Qian et al. 2016). Sialylation of the mature glycosylated UT-A3 by sialyltransferase increases protein stability, cell surface expression, and urea transport activity via a PKA pathway (Qian et al. 2016).

UT-B1

UT-B1 is expressed in red blood cells (Olives et al. 1995) and the endothelial cells of the DVR (Fig. 6), and is phloretin inhibitable (Lim et al. 2006; Xu et al. 1997). The AVR lack UT-B1 but are fenestrated and thus permeable to urea (Kriz, 1981; Pallone et al. 2012). The AVR take up urea that is delivered to the IM from the CDs into the plasma and red blood cells and much of this urea is then recycled back to the IM by re-entering the DVR via UT-B1 or the DTLs via UT-A2 (Yang and Bankir 2005; Pallone et al. 2012). *UT-B* knockouts display impaired urea recycling with increased blood urea and decreased urinary urea (Yang et al. 2002).

Regulation of UT-B1

Brattleboro rats treated chronically with dDAVP or AVP have increased *UT-B1* mRNA in the OM and the IM base, but decreased *UT-B1* mRNA in the IM tip (Promeneur et al. 1998). A study by Trinh-Trang-Tan et al. (2002) confirmed that protein expression of UT-B1 in the IM of Sprague-Dawley rats decreased after long-term infusion of dDAVP. Compared to controls, UT-B1 protein in the medulla (inner and outer combined) was higher in dehydrated rats and lower in hydrated rats (Lim et al. 2006). More recently, Wang et al. (2016b) suggested that miRNA (miR-200c) may have a role in the regulation of UT-B1 expression. They examined the IM and OM of dehydrated mice and reported that miR-200c increased and UT-B1 protein abundance decreased in the IM while in the OM, miR-200c decreased and UT-B1 protein increased.

Urea Transporter Variants and Alternatives

Studies in the chinchilla (Chou and Knepper, 1992, 1993) and Munich-Wistar rat (Nawata et al. 2014) show high urea permeability in the inner medullary thin limb segments where no known urea transporters have been identified. The mRNA of *UT-A2* variants and the sodium-glucose transporters *SGLT1a (Slc5A1)* and *NAGLT1* (*Slc59A2*) were identified in the thin limbs in the IM of the Munich-Wistar rat (Nawata et al. 2015). These transcripts were modulated by water restriction and their proteins facilitated urea transport when expressed in *Xenopus* oocytes. It is not known if these or other transporters that transport urea, like AQPs (Li and Wang 2014), transport urea in vivo. The possibility that other transcellular or paracellular urea pathways exist in the IM can also not be ruled out.

Sodium Transporters in the TAL

NKCC2—The reabsorption of NaCl by the TALs serves to dilute the TAL fluid as well as generate an osmotic gradient in the OM (Burg 1982). The TAL reclaims 15-20% of the NaCl filtered at the glomerulus (Hebert and Andreoli 1984) and NKCC2 serves as the major entry point for NaCl in the TAL (Greger and Velazquez 1987). The importance of NKCC2 in salt reabsorption and urine concentration is demonstrated in Barrter's syndrome type I. Mutations of NKCC2 prevent or reduce salt reabsorption from the TALs causing severe polyuria and salt-wasting, among other symptoms (Bartter et al. 1998; Castrop and Scheiß1 2014).

NKCC2 is located in the apical plasma membrane and subapical intracellular vesicles of the TAL (Nielsen et al. 1998) (Fig. 6). Na^+ and Cl^- that enter via NKCC2 leave the basolateral membrane through Na^+-K^+-ATPase and the basolateral chloride channel and K^+-Cl^- cotransporter 4, while apical K^+ is recycled via renal outer medullary K^+ channels and Ca^{++}-activated maxi K^+ channels (Mount 2014) (Fig. 8).

Apical membrane NKCC2 levels are kept at steady state by endocytosis, exocytic delivery and recycling (Ares et al. 2011). Vesicle-associated membrane protein 2 mediates cAMP-stimulated NKCC2 exocytotic delivery and surface expression in the TALs, and constitutive exocytotic delivery is mediated by vesicle-associated membrane protein 3 (Caceres et al. 2016).

NKCC2 is regulated by a number of hormones and mediators (reviewed by Castrop and Schieß1 2014; Mount 2014) but AVP is the most studied regulator (e.g. Bertuccio et al. 2002; Kim et al. 1999; Knepper et al. 1999; Kortenoeven et al. 2015). AVP has both short-term and long-term effects on NKCC2. Acute application of AVP increases NaCl transport (Besseghir et al. 1986) and increases total NKCC2 abundance without increasing mRNA levels (Mutig et al. 2007). It also enhances phosphorylation (Gunaratne et al. 2010; Mutig et al. 2007) which is mediated by adenylyl cyclase 6 (Reig et al. 2013), and stimulates the exocytosis of NKCC2 proteins from subapical vesicles to the plasma membrane (Ares et al. 2011). Water restriction increases abundance of NKCC2 as does dDAVP infusion in Brattleboro rats (Kim et al. 1999). Transgenic suppression of AVP-V2R signaling in rats decreases NKCC2 abundance, phosphorylation, and surface expression in the TAL (Mutig et al. 2016). Additionally, these rats lacking AVP-V2R signaling have baseline polyuria and a urine-concentrating defect in response to water deprivation.

NHE3—Na^+/H^+ exchanger 3 (NHE3) is expressed in the apical membrane of the TALs where it mediates bicarbonate reabsorption (Amemiya et al. 1995; Mount 2014). *NHE3* knockout studies also indicate a role for NHE3 in urine concentration (Fenton et al. 2017). NHE3 therefore serves as a possible alternate entry point for Na^+ into the TAL (Knepper et al. 1999). However, Na^+ also enters paracellular pathways (Fig. 8) in the TAL epithelium in order to balance Na^+ and Cl^- transport (Hebert and Andreoli 1984; Mount 2014). NHE3 activity is decreased by AVP (Good 1990) which results from the inhibitory effect of phosphorylation at S552 (Gunaratne et al. 2010; Zhao et al. 1999).

Na^+-K^+-ATPase—Na^+-K^+-ATPase is responsible for net Na^+ reabsorption in the kidney as demonstrated in a study by Garg et al. (1981) that showed good correlation between Na^+-K^+-ATPase activity and net Na^+ transport rate in different nephron tubule segments including the TAL. Short-term administration of AVP, cAMP analogs, or forskolin stimulate Na^+-K^+-ATPase in the medullary TAL (Kiroytcheva et al. 1999; Kortenoeven et al. 2015). Dehydration increases Na^+-K^+-ATPase activity in the medullary TAL of rats as does acute exposure of the TALs to a hypertonic medium (Sakuma et al. 2005). Inhibition of V2R results in decreased activity and expression of Na^+-K^+-ATPase in the OM of rats (Bertuccio et al. 2002).

CONCLUSION AND PERSPECTIVES

Although our understanding of urine concentration is not yet complete, modeling and imaging studies are elucidating the role of medullary architecture, and molecular investigations are revealing the mechanisms involved in membrane transport. Recently, Chou et al. (2018) identified proteins that interact with AQP2 and UT-A1 in rat IMCD cells. Interactomes like these as well as transcriptomes of individual cell types like that recently described for mouse CDs by Chen et al. (2017) will provide further information that can be incorporated into mathematical models. The role of paracellular transport is also gaining attention with recent studies highlighting roles for a paracellular Na^+ permeation pathway in the ATLs (Sonntag et al. 2018) and paracellular water permeation in the TALs (Gong et al. 2017). These types of studies as well as others that embrace a greater variety of animal species will provide further insights into the workings of urine concentration in mammals.

Acknowledgments

This research was supported by the National Institute of Diabetes and Digestive and Kidney Diseases grant DK083338, National Science Foundation Grant IOS-0952885 and Joint DMS/NIGMS Initiative under NSF grant DMS-1263943.

LIST OF ABBREVIATIONS

AQP	aquaporin
AMPK	adenosine monophosphate kinase
ATL	ascending thin limb
AVP	arginine vasopressin
AVR	ascending vasa recta
CD	collecting duct
dDAVP	desmopressin
DTL	descending thin limb
DVR	descending vasa recta
Epac	exchange protein activated by cAMP
IM	inner medulla
IMCD	inner medullary collecting duct
ISOM	inner stripe of the outer medulla
LXR	liver X receptor
NHE3	Na^+/H^+ exchanger 3
NKCC2	Na^+-K^+-$2Cl^-$ cotransporter 2
OM	outer medulla
OSOM	outer stripe of the outer medulla
$P2Y_{12}$-R	purinergic $P2Y_{12}$ receptor
PGE_2	prostaglandin E2
PRR	prorenin receptor
sPRR	soluble prorenin receptor
STZ	streptozotocin
TAL	thick ascending limb
UT	urea transporter

V2R	arginine vasopressin receptor 2

References

Advani A, Kelly DJ, Cox AJ, White KE, Advani SL, Thai K, Connelly KA, Yuen D, Trogadis J, Herzenberg AM, Kuliszewski MA, Leong-Poi H, Gilbert RE. The (pro)renin receptor: site-specific and functional linkage to the vacuolar H^+-ATPase in the kidney. Hypertension. 2009; 54:261–269. [PubMed: 19546380]

Al-bataineh MM, Li H, Ohmi K, Gong F, Marciszyn AL, Naveed S, Zhu X, Neumann D, Wu Q, Cheng L, Fenton RA, Pastor-Soler NM, Hallows KR. Activation of the metabolic sensor AMP-activated protein kinase inhibits aquaporin-2 function in kidney principal cells. Am J Physiol. 2016; 311:F890–F900.

Amemiya M, Loffing J, Lotscher M, Kaissling B, Alpern RJ, Moe OW. Expression of NHE-3 in the apical membrane of rat renal proximal tubule and thick ascending limb. Kidney Int. 1995; 48:1206–1215. [PubMed: 8569082]

Ares GR, Caceres PS, Ortiz PA. Molecular regulation of NKCC2 in the thick ascending limb. Am J Physiol. 2011; 301:F1143–F1159.

Arystarkhova E, Bouley R, Liu YB, Sweadner KJ. Impaired AQP2 trafficking in *Fyxd1* knockout mice: a role for FYXD1 in regulated vesicular transport. PLoS ONE. 2017; 12(11):e0188006. [PubMed: 29155857]

Aw M, Armstrong TM, Nawata CM, Bodine SN, Oh JJ, Wei G, Evans KK, Shahidullah M, Rieg T, Pannabecker TL. Body mass-specific Na^+, K^+-ATPase activity in the medullary thick ascending limb - implications for species-dependent urine concentrating mechanisms. J Am Physiol. 2018; doi: 10.1152/ajpregu.00289.2017

Bachmann S, Kriz W. Histotopography and ultrastructure of the thin limbs of the loop of Henle in the hamster. Cell Tissue Res. 1982; 225:111–127. [PubMed: 6889464]

Bagnasco SM, Peng T, Nakayama Y, Sands JM. Differential expression of individual UT-A urea transporter isoforms in rat kidney. J Am Soc Nephrol. 2000; 11:1980–1986. [PubMed: 11053472]

Bagnasco SM, Peng T, Janech MG, Karakashian A, Sands JM. Cloning and characterization of the human urea transporter UT-A1 and mapping of the human Slc14a2 gene. Am J Physiol. 2001; 281:F400–F406.

Bai JJ, Tan CD, Chow BKC. Secretin, at the hub of water-salt homeostasis. Am J Physiol. 2017; 312:F852–F860.

Bankir L, De Rouffignac C. Urinary concentrating ability: insights from comparative anatomy. Am J Physiol. 1985; 249:R643–R666. [PubMed: 3934988]

Bankir L, Kriz W. Adaptation of the kidney to protein intake and to urine concentrating activity: similar consequences in health and CRF. Kidney Int. 1995; 47:7–24. [PubMed: 7731172]

Bardoux P, Ahloulay M, Le Maout S, Bankir L, Trinh-Trang-Tan M-M. Aquaporin-2 and urea transporter-A1 are up-regulated in rats with type I diabetes mellitus. Diabetologia. 2001; 44:637–645. [PubMed: 11380083]

Bartel DP. MicroRNAs: genomics, biogenesis, mechanism, and function. Cell. 2004; 116:281–297. [PubMed: 14744438]

Bartter FC, Pronove P, Gill JR Jr, MacCardle RC. Hyperplasia of the juxtaglomerular complex with hyperaldosteronism and hypokalemic alkalosis. A new syndrome. 1962. J Am Soc Nephrol. 1998; 9:516–528. [PubMed: 9513916]

Bertuccio CA, Ibarra FR, Toledo JE, Arrizurieta EE, Martin RS. Endogenous vasopressin regulates Na-K-ATPase and Na^+-K^+-Cl^- cotransporter *rbsc-1* in rat outer medulla. Am J Physiol. 2002; 282:F265–F270.

Besseghir K, Trimble ME, Stoner L. Action of ADH on isolated medullary thick ascending limb of the Brattleboro rat. Am J Physiol. 1986; 251:F271–F277. [PubMed: 3740274]

Beuchat CA. Structure and concentrating ability of the mammalian kidney: correlations with habitat. Am J Physiol. 1996; 271:R157–R179. [PubMed: 8760217]

Blount MA, Klein JD, Martin CF, Tchapyjnikov D, Sands JM. Forskolin stimulates phosphorylation and membrane accumulation of UT-A3. Am J Physiol. 2007; 293:F1308–F1313.

Blount MA, Mistry AC, Frohlich O, Price SR, Chen G, Sands JM, Klein JD. Phosphorylation of UT-A1 urea transporter at serines 486 and 499 is important for vasopressin-regulated activity and membrane accumulation. Am J Physiol. 2008; 295:F295–F299.

Blount MA, Cipriani P, Redd SK, Ordas RJ, Black LN, Gumina DL, Hoban CA, Klein JD, Sands JM. Activation of protein kinase C increases phosphorylation of the UT-A1 urea transporter at serine 494 in the inner medullary collecting duct. Am J Physiol. 2015; 309:C608–C615.

Boone M, Deen PMT. Physiology and pathophysiology of the vasopressin-regulated renal water reabsorption. Pflugers Arch. 2008; 456:1005–1024. [PubMed: 18431594]

Burg MB. Thick ascending limb of Henle's loop. Kidney Int. 1982; 22:454–464. [PubMed: 6296522]

Caceres PS, Mendez M, Haque MZ, Ortiz PA. Vesicle-associated membrane protein 3 (VAMP3) mediates constitutive trafficking of the renal co-transporter NKCC2 in thick ascending limbs: role in renal function and blood pressure. J Biol Chem. 2016; 291:22063–22073. [PubMed: 27551042]

Cano-Penalver JL, Griera M, Serrano I, Rodríguez-Puyol D, Dedhar S, de Frutos S, Rodríguez-Puyol M. Integrin-linked kinase regulates tubular aquaporin-2 content and intracellular location: a link between the extracellular matrix and water reabsorption. FASEB J. 2014; 28:3645–3659. [PubMed: 24784577]

Castrop H, Schieß1 IM. Physiology and pathophysiology of the renal Na-K-2Cl cotransporter (NKCC2). Am J Physiol. 2014; 307:F991–F1002.

Centrone M, Ranieri M, Di Mise A, Berlingerio SP, Russo A, Deen PMT, Staub O, Valenti G, Tamma G. AQP2 abundance is regulated by the E3-ligase CHIP via HSP70. Cell Physiol Biochem. 2017; 44:515–531. [PubMed: 29145196]

Chen J, Edwards A, Layton AT. A mathematical model of O2 transport in the rat outer medulla. II. Impact of outer medullary architecture. Am J Physiol. 2009a; 297:F537–F548.

Chen J, Edwards A, Layton AT. Effects of pH and medullary blood flow on oxygen transport and sodium reabsorption in the rat outer medulla. Am J Physiol. 2010; 298:F1369–F1383.

Chen J, Layton AT, Edwards A. A mathematical model of oxygen transport in the rat outer medulla: I. Model formulation and baseline results. Am J Physiol. 2009b; 297:F537–F548.

Chen L, Lee JW, Chou CL, Nair AV, Battistone MA, Paunescu TG, Merkulova M, Breton S, Verlander JW, Wall SM, Brown D, Burg MB, Knepper MA. Transcriptomes of major renal collecting duct cell types in mouse identified by single-cell RNA-seq. Proc Natl Acad Sci. 2017; 114:9989–9998.

Chou CL, Knepper MA. In vitro perfusion of chinchilla thin limb segments: segmentation and osmotic water permeability. Am J Physiol. 1992; 263:F417–F426. [PubMed: 1415570]

Chou CL, Knepper MA. In vitro perfusion of chinchilla thin limb segments: urea and NaCl permeabilities. Am J Physiol. 1993; 264:F337–F343. [PubMed: 8447443]

Chou CL, Nielsen S, Knepper MA. Structural-functional correlation in chinchilla long loop of Henle thin limbs: a novel papillary subsegment. Am J Physiol. 1993; 265:F863–F874. [PubMed: 7506872]

Chou CL, Ma T, Yang B, Knepper MA, Verkman AS. Fourfold reduction of water permeability in inner medullary collecting duct of aquaporin-4 knockout mice. Am J Physiol. 1998; 274:C549–C554. [PubMed: 9486146]

Chou CL, Hwang G, Hageman DJ, Han L, Agrawal P, Pisitkun T, Knepper MA. Identification of UT-A1 and AQP2 interacting proteins in rat inner medullary collecting duct. Am J Physiol. 2018; 314:C99–C117.

Christensen EI, Grann B, Kristoffersen IB, Skriver E, Thomsen JS, Andreasen A. Three-dimensional reconstruction of the rat nephron. Am J Physiol. 2014; 306:F664–671.

Christensen EI, Wagner CA, Kaissling B. Uriniferous tubule: structural and functional organization. Compr Physiol. 2012; 2:805–861. [PubMed: 23961562]

Clapp WL, Madsen KM, Verlander JW, Tisher CC. Morphologic heterogeneity along the rat inner medullary collecting duct. Lab Invest. 1989; 60:219–230. [PubMed: 2915516]

Cousin C, Bracquart D, Contrepas A, Corvol P, Muller L, Nguyen G. Soluble form of the (pro)renin receptor generated by intracellular cleavage by furin is secreted in plasma. Hypertension. 2009; 53:1077–1082. [PubMed: 19380613]

Dantzler WH, Layton AT, Layton HE, Pannabecker TL. Urine-concentrating mechanism in the inner medulla: function of the thin limbs of the loops of Henle. Clin J Am Nephrol. 2014; 9:1781–1789.

Dikic I, Robertson M. Ubiquitin ligases and beyond. BMC Biology. 2012; 10:22. [PubMed: 22420755]

Dorsam RT, Kunapuli SP. Central role of the $P2Y_{12}$ receptor in platelet activation. J Clin Invest. 2004; 113:340–345. [PubMed: 14755328]

Ecelbarger CA, Terris J, Frindt G, Echevarria M, Marples D, Nielsen S, Knepper MA. Aquaporin-3 water channel localization and regulation in rat kidney. Am J Physiol. 1995; 269:F663–F672. [PubMed: 7503232]

Fenton RA, Knepper MA. Mouse models and the urinary concentrating mechanism in the new millennium. Physiol Rev. 2007; 87:1083–1112. [PubMed: 17928581]

Fenton RA, Cottingham CA, Stewart GS, Howorth A, Hewitt JA, Smith CP. Structure and characterization of the mouse UT-A gene (*Slc14a2*). Am J Physiol. 2002a; 282:F630–F638.

Fenton RA, Stewart GS, Carpenter B, Howorth A, Potter EA, Cooper GJ, Smith CP. Characterization of mouse urea transporters UT-A1 and UT- A2. Am J Physiol. 2002b; 283:F817–F825.

Fenton RA, Chou CL, Stewart GS, Smith CP, Knepper MA. Urinary concentrating defect in mice with selective deletion of phloretin-sensitive urea transporters in the renal collecting duct. Proc Natl Acad Sci. 2004; 101:7469–7474. [PubMed: 15123796]

Fenton RA, Poulsen SB, de la Mora Chavez S, Soleimani M, Dominguez Rieg JA, Rieg T. Renal tubular NHE_3 is required in the maintenance of water and sodium chloride homeostasis. Kidney Int. 2017; 92:397–414. [PubMed: 28385297]

Fenton RA, Yang B. Urea transporter knockout mice and their renal phenotypes. Subcell Biochem. 2014; 73:137–152. [PubMed: 25298343]

Franchini KG, Cowley AW Jr. Sensitivity of the renal medullary circulation to plasma vasopressin. Am J Physiol. 1996; 271:R647–R653. [PubMed: 8853387]

Frigeri A, Gropper MA, Turck CW, Verkman AS. Immunolocalization of the mercurial-insensitive water channel and glycerol intrinsic protein in epithelial cell plasma membranes. Proc Natl Acad Sci. 1995; 92:4328–4331. [PubMed: 7538665]

Fry BC, Edwards A, Sgouralis I, Layton AT. Impact of renal medullary three-dimensional architecture on oxygen transport. Am J Physiol. 2014; 307:F263–272.

Gamble JL, McKhann CF, Butler AM, Tuthill E. An economy of water in renal function referable to urea. Am J Physiol. 1934; 109:139–154.

Garg LC, Knepper MA, Burg MB. Mineralocorticoid effects on Na-K-ATPase in individual nephron segments. Am J Physiol. 1981; 240:F536–F544. [PubMed: 6264796]

Geering K. FXYD proteins: new regulators of Na-K-ATPase. Am J Physiol. 2006; 290:F241–F250.

Gong Y, Himmerkus N, Sunq A, Milatz S, Merkel C, Bleich M, Hou J. ILDR1 is important for paracellular water transport and urine concentration mechanism. Proc Natl Acad Sci. 2017; 114:5271–5276. [PubMed: 28461473]

Good DW. Inhibition of bicarbonate absorption by peptide hormones and cyclic adenosine monophosphate in rat medullary thick ascending limb. J Clin Invest. 1990; 85:1006–1013. [PubMed: 2318960]

Gottschalk CW, Mylle M. Micropuncture study of the mammalian urinary concentrating mechanism: evidence for the countercurrent hypothesis. Am J Physiol. 1959; 196:927–936. [PubMed: 13637248]

Greger R, Velazquez H. The cortical thick ascending limb and early distal convoluted tubule in the urinary concentrating mechanism. Kidney Int. 1987; 31:590–596. [PubMed: 3550228]

Gunaratne R, Braucht DWW, Rinschen MM, Chou CL, Hoffert JD, Pisitkun T, Knepper MA. Quantitative phosphoproteomic analysis reveals cAMP/vasopressin-dependent signaling pathways in native renal thick ascending limb cells. Proc Natl Acad Sci. 2010; 107:15653–15658. [PubMed: 20713729]

Hasler U, Leroy V, Martin P-Y, Feraille E. Aquaporin-2 abundance in the renal collecting duct: new insights from cultured cell models. Am J Physiol. 2009; 297:F10–F18.

Hassouneh R, Nasrallah R, Zimpelmann J, Gutsol A, Eckert D, Ghossein J, Burns KD, Hebert RL. PGE_2 receptor EP_3 inhibits water reabsorption and contributes to polyuria and kidney injury in a

streptozotocin-induced mouse model of diabetes. Diabetologia. 2016; 59:1318–1328. [PubMed: 26995650]

Hebert SC, Andreoli TE. Control of NaCl transport in the thick ascending limb. Am J Physiol. 1984; 246:F745–F756. [PubMed: 6377912]

Hervy S, Thomas SR. Inner medullary lactate production and urine-concentrating mechanism: a flat medullary model. Am J Physiol. 2003; 284:F65–F81.

Hoban CA, Black LN, Ordas RJ, Gumina DL, Pulous FE, Sim JH, Sands JM, Blount MA. Vasopressin regulation of multisite phosphorylation of UT-A1 in the inner medullary collecting duct. Am J Physiol. 2015; 308:F49–F55.

Imai M, Hayashi M, Araki M. Functional heterogeneity of the descending limbs of Henle's loop. I. Internephron heterogeneity in the hamster kidney. Pflugers Arch. 1984; 402:385–392. [PubMed: 6522245]

Ishibashi K, Sasaki S, Fushimi K, Uchida S, Kuwahara M, Saito H, Furukawa T, Nakajima K, Yamaguchi Y, Gojobori T, Marumo F. Molecular cloning and expression of a member of the aquaporin family with permeability to glycerol and urea in addition to water expressed at the basolateral membrane of kidney collecting duct cells. Proc Natl Acad Sci. 1994; 91:6269–6273. [PubMed: 7517548]

Issaian T, Urity VB, Dantzler WH, Pannabecker TL. Architecture of vasa recta in the renal inner medulla of the desert rodent Dipodomys merriami: potential impact on the urine concentrating mechanism. Am J Physiol. 2012; 302:R748–R756.

Jamison RL, Gehrig JJ, Jr. Urinary concentration and dilution: physiology. In: Terjung R, editorHandbook of physiology, renal physiology. Am Physiol Soc. Bethesda; 2011. 1219–1279.

Jamison RL, Kriz W. Urinary concentrating mechanism. Oxford University Press; New York: 1982.

Jen JF, Stephenson JL. Externally driven countercurrent multiplication in a mathematical model of the urinary concentrating mechanism of the renal inner medulla. Bull Math Biol. 1994; 56:491–514. [PubMed: 8087079]

Jiang T, Li Y, Layton AT, Wang W, Sun Y, Li M, Zhou H, Yang B. Generation and phenotypic analysis of mice lacking all urea transporters. Kidney Int. 2017; 91:338–351. [PubMed: 27914708]

Jung HJ, Kwon T-H. Molecular mechanisms regulating aquaporin-2 in kidney collecting duct. Am J Physiol. 2016; 311:F1318–F1328.

Kaissling B, Kriz W. Morphology of the loop of Henle, distal tubule, and collecting duct. In: Windhager EE, editorHandbook of physiology, Sec 8, Renal physiology. Oxford University Press; New York: 1992. 109–167.

Karakashian A, Timmer RT, Klein JD, Gunn RB, Sands JM, Bagnasco SM. Cloning and characterization of two new isoforms of the rat kidney urea transporter: UT-A3 and UT-A4. J Am Soc Nephrol. 1999; 10:230–237. [PubMed: 10215321]

Kim D, Sands JM, Klein JD. Changes in renal medullary transport proteins during uncontrolled diabetes mellitus in rats. Am J Physiol. 2003; 285:F303–F309.

Kim G-H, Ecelbarger CA, Mitchell C, Packer RK, Wade JB, Knepper MA. Vasopressin increases Na-K-2Cl cotransporter expression in thick ascending limb of Henle's loop. Am J Physiol. 1999; 276:F96–F103. [PubMed: 9887085]

Kim J, Pannabecker TL. Two-compartment model of inner medullary vasculature supports dual modes of vasopressin-regulated inner medullary blood flow. Am J Physiol. 2010; 299:F273–F279.

Kim J-E, Jung HJ, Lee Y-J, Kwon T-H. Vasopressin-regulated miRNAs and AQP2-targeting miRNAs in kidney collecting duct cells. Am J Physiol. 2015; 308:F749–F764.

King LS, Choi M, Fernandez PC, Cartron J-P, Agre P. Defective urinary concentrating ability due to a complete deficiency of aquaporin-1. N Engl J Med. 2001; 345:175–179. [PubMed: 11463012]

Kiroytcheva M, Cheval L, Carranza ML, Martin P-Y, Favre H, Doucet A, Feraille E. Effect of cAMP on the activity and the phosphorylation of Na^+, K^+-ATPase in rat thick ascending limb of Henle. Kidney Int. 1999; 55:1819–1831. [PubMed: 10231444]

Klein JD. Expression of urea transporters and their regulation. Subcell Biochem. 2014; 73:79–108. [PubMed: 25298340]

Klein JD, Martin CF, Kent KJ, Sands JM. Protein kinase C-mediates hypertonicity-stimulated increase in urea transporter phosphorylation in the inner medullary collecting duct. Am J Physiol. 2012; 302:F1098–F1103.

Klein JD, Sands JM. Urea transport and clinical potential of urearetics. Curr Opin Nephrol Hypertens. 2016; 25:444–451. [PubMed: 27367911]

Klein JD, Wang Y, Blount MA, Molina PA, LaRocque LM, Ruiz JA, Sands JM. Metformin, an AMPK activator, stimulates the phosphorylation of aquaporin 2 and urea transporter A1 in inner medullary collecting ducts. Am J Physiol. 2016a; 310:F1008–F1012.

Klein JD, Wang Y, Mistry A, LaRocque LM, Molina PA, Rogers RT, Blount MA, Sands JM. Transgenic restoration of urea transporter A1 confers maximal urinary concentration in the absence of urea transporter A3. J Am Soc Nephrol. 2016b; 27:1448–1455. [PubMed: 26407594]

Knepper MA. Measurement of osmolality in kidney slices using vapor pressure osmometry. Kidney Int. 1982; 21:653–655. [PubMed: 7098276]

Knepper MA, Kim G-H, Fernandez-Llama P, Ecelbarger CA. Regulation of thick ascending limb transport by vasopressin. J Am Soc Nephrol. 1999; 10:628–634. [PubMed: 10073614]

Knepper MA, Roch-Ramel F. Pathways of urea transport in the mammalian kidney. Kidney Int. 1987; 31:629–633. [PubMed: 3550233]

Knepper MA, Saidel GM, Hascall VC, Dwyer T. Concentration of solutes in the renal inner medulla: interstitial hyaluronan as a mechano-osmotic transducer. Am J Physiol. 2003; 284:F433–F446.

Kokko JP, Rector FC Jr. Countercurrent multiplication system without active transport in inner medulla. Kidney Int. 1972; 2:214–223. [PubMed: 4657922]

Kone BC, Madsen KM, Tisher CC. Ultrastructure of the thick ascending limb of Henle in the rat kidney. Am J Anat. 1984; 171:217–226. [PubMed: 6496376]

Kortenoeven MLA, Pedersen NB, Rosenbaek LL, Fenton RA. Vasopressin regulation of sodium transport in the distal nephron and collecting duct. Am J Physiol. 2015; 309:F280–F299.

Kriz W. Structural organization of the renal medulla: comparative and functional aspects. Am J Physiol. 1981; 241:R3–R16. [PubMed: 7018270]

Kriz W. Structural organization of renal medullary circulation. Nephron. 1982; 31:290–295. [PubMed: 7177264]

Kuhn W, Ryffel K. Herstellung konzentrierter losüngen aus verdünten durch blosse membranwirkung: ein modellversuch zur funktion der niere. Hoppe-Seylers Z Physiol Chem. 1942; 276:145–178.

Lam AKM, Ko BCB, Tam S, Morris R, Yang JY, Chung SK, Chung SMS. Osmotic response element-binding protein (OREBP) is an essential regulator of the urine concentrating mechanism. J Biol Chem. 2004; 279:48048–48054. [PubMed: 15347663]

Lassiter WE, Gottschalk CW, Mylle M. Micropuncture study of net transtubular movement of water and urea in nondiuretic mammalian kidney. Am J Physiol. 1961; 200:1139–1146. [PubMed: 13759324]

Layton AT. A mathematical model of the urine concentrating mechanism in the rat renal medulla: II. Functional implications of three-dimensional architecture. Am J Physiol. 2011; 300:F372–F384.

Layton AT, Gilbert RL, Pannabecker TL. Isolated interstitial nodal spaces may facilitate preferential solute and fluid mixing in the rat renal inner medulla. Am J Physiol. 2012; 302:F830–F839.

Layton AT, Layton HE. Countercurrent multiplication may not explain the axial osmolality gradient in the outer medulla of the rat kidney. Am J Physiol. 2011; 301:F1047–F1056.

Layton AT, Layton HE, Dantzler WH, Pannabecker TL. The mammalian urine concentrating mechanism: hypotheses and uncertainties. Physiology. 2009; 24:250–256. [PubMed: 19675356]

Layton AT, Pannabecker TL, Dantzler WH, Layton HE. Two modes for concentrating urine in the rat inner medulla. Am J Physiol. 2004; 287:F816–F839.

Layton AT, Pannabecker TL, Dantzler WH, Layton HE. Functional implications of the three-dimensional architecture of the rat renal inner medulla. Am J Physiol. 2010; 298:F973–F987.

Lee Y-J, Song I-K, Jang K-J, Nielsen J, Frokiaer J, Nielsen S, Kwon T-H. Increased AQP2 targeting in primary cultured IMCD cells in response to angiotensin II through AT_1 receptor. Am J Physiol. 2007; 292:F340–F350.

Lei T, Zhou L, Layton AT, Zhou H, Zhao X, Bankir L, Yang B. Role of thin descending limb urea transport in renal urea handling and the urine concentrating mechanism. Am J Physiol. 2011; 301:F1251–F1259.

Lemley KV, Kriz W. Cycles and separations: the histotopography of the urinary concentrating process. Kidney Int. 1987; 31:538–548. [PubMed: 3550222]

Lemley KV, Kriz W. Anatomy of the renal interstitium. Kidney Int. 1991; 39:370–381. [PubMed: 2062030]

Li C, Wang W. Urea transport mediated by aquaporin water channel proteins. Subcell Biochem. 2014; 73:227–265. [PubMed: 25298348]

Li X, Chen G, Yang B. Urea transporter physiology studied in knockout mice. Front Physiol. 2012; 3:217. [PubMed: 22745630]

Li Y, Wei Y, Zheng F, Guan Y, Zhang X. Prostaglandin E2 in the regulation of water transport in renal collecting ducts. Int J Mol Sci. 2017; 18:2539.

Lim S-W, Han K-H, Jung J-Y, Kim W-Y, Yang C-W, Sands JM, Knepper MA, Madsen KM, Kim J. Ultrastructural localization of UT-A and UT-B in rat kidneys with different hydration status. Am J Physiol. 2006; 290:R479–R492.

Lu X, Wang F, Xu C, Soodvilai S, Peng K, Su J, Zhao L, Yang KT, Feng Y, Zhou S-F, Gustafsson J-A, Yang T. Soluble (pro)renin receptor via β-catenin enhances urine concentration capability as a target of liver X receptor. Proc Natl Acad Sci. 2016; 113:E1898–E1906. [PubMed: 26984496]

Luo Y, Liu Y, Liu M, Wei J, Zhang Y, Hou J, Huang W, Wang T, Li X, He Y, Ding F, Yuan L, Cai J, Zheng F, Tang JY. *Sfmbt2* 10th intron-hosted miR-466(a/e)-3p are important epigenetic regulators of Nfat5 signaling, osmoregulation and urine concentration in mice. Biochim Biophys Acta. 2014; 1839:97–106. [PubMed: 24389345]

Ma T, Frigeri A, Hasegawa H, Verkman AS. Cloning of a water channel homolog expressed in brain meningeal cells and kidney collecting duct that functions as a stilbene-sensitive glycerol transporter. J Biol Chem. 1994; 269:21845–21849. [PubMed: 8063828]

Ma T, Yang B, Gillespie A, Carlson EJ, Epstein CJ, Verkman AS. Generation and phenotype of a transgenic knockout mouse lacking the mercurial-insensitive water channel aquaporin-4. J Clin Invest. 1997; 100:957–962. [PubMed: 9276712]

Ma T, Yang B, Gillespie A, Carlson EJ, Epstein CJ, Verkman AS. Severely impaired urinary concentrating ability in transgenic mice lacking aquaporin-1 water channels. J Biol Chem. 1998; 273:4296–4299. [PubMed: 9468475]

Ma T, Song Y, Yang B, Gillespie A, Carlson EJ, Epstein CJ, Verkman AS. Nephrogenic diabetes insipidus in mice lacking aquaporin-3 water channels. Proc Natl Acad Sci. 2000; 97:4386–4391. [PubMed: 10737773]

MacPhee PJ, Michel CC. Fluid uptake from the renal medulla into the ascending vasa recta in anaesthetized rats. J Physiol. 1995; 487:169–183. [PubMed: 7473246]

Madsen KM, Clapp WL, Verlander JW. Structure and function of the inner medullary collecting duct. Kidney Int. 1988; 34:441–454. [PubMed: 3059025]

Marples D, Christensen S, Christensen EI, Ottosen PD, Nielsen S. Lithium-induced downregulation of aquaporin-2 water channel expression in rat kidney medulla. J Clin Invest. 1995; 95:1838–1845. [PubMed: 7535800]

Michalek K. Aquaglyceroporins in the kidney: present state of knowledge and prospects. J Physiol Pharmacol. 2016; 67:185–193. [PubMed: 27226178]

Michel CC, Curry FE. Microvascular permeability. Physiol Rev. 1999; 79:703–761. [PubMed: 10390517]

Moffat DB, Fourman J. The vascular pattern of the rat kidney. J Anat. 1963; 97:543–553. [PubMed: 14064096]

Mount DB. Thick ascending limb of the loop of Henle. Clin J Am Soc Nephrol. 2014; 9:1974–1986. [PubMed: 25318757]

Mutig K, Paliege A, Kahl T, Jons T, Muller-Esterl W, Bachmann S. Vasopressin V_2 receptor expression along rat, mouse, and human renal epithelia with focus on TAL. Am J Physiol. 2007; 293:F1166–F1177.

Mutig K, Borowski T, Boldt C, Borschewski A, Paliege A, Popova E, Bader M, Bachmann S. Demonstration of the functional impact of vasopressin signaling in the thick ascending limb by a targeted transgenic rat approach. Am J Physiol. 2016; 311:F411–F423.

Nawata CM, Evans KK, Dantzler WH, Pannabecker TL. Transepithelial water and urea permeabilities of isolated perfused Munich-Wistar rat inner medullary thin limbs of Henle's loop. Am J Physiol. 2014; 306:F123–F129.

Nawata CM, Dantzler WH, Pannabecker TL. Alternative channels for urea in the inner medulla of the rat kidney. Am J Physiol. 2015; 309:F916–F924.

Nejsum LN, Kwon T-H, Marples D, Flyvbjerg A, Knepper MA, Frokiaer J, Nielsen S. Compensatory increase in AQP2, p-AQP2, and AQP3 expression in rats with diabetes mellitus. Am J Physiol. 2001; 280:F715–F726.

Nguyen G, Delarue F, Burckle C, Bouzhir L, Giller T, Sraer J-D. Pivotal role of the renin/prorenin receptor in angiotensin II production and cellular responses to renin. J Clin Invest. 2002; 109:1417–1427. [PubMed: 12045255]

Nielsen S, DiGiovanni SR, Christensen EI, Knepper MA, Harris HW. Cellular and subcellular immunolocalization of vasopressin-regulated water channel in rat kidney. Proc Natl Acad Sci. 1993; 90:11663–11667. [PubMed: 8265605]

Nielsen S, Pallone T, Smith BL, Christensen EI, Agre P, Maunsbach AB. Aquaporin-1 water channels in short and long loop descending thin limbs and in descending vasa recta in rat kidney. Am J Physiol. 1995; 268:F1023–1037. [PubMed: 7541952]

Nielsen S, Terris J, Smith CP, Hediger MA, Ecelbarger CA, Knepper MA. Cellular and subcellular localization of the vasopressin-regulated urea transporter in rat kidney. Proc Natl Acad Sci. 1996; 93:5495–5500. [PubMed: 8643603]

Nielsen S, Maunsbach AB, Ecelbarger CA, Knepper MA. Ultrastructural localization of Na-K-2Cl cotransporter in thick ascending limb and macula densa of rat kidney. Am J Physiol. 1998; 275:F885–F893. [PubMed: 9843905]

Nielsen S, Frokiaer J, Marples D, Kwon T-H, Agre P, Knepper MA. Aquaporins in the kidney: from molecules to medicine. Physiol Rev. 2002; 82:205–244. [PubMed: 11773613]

Olesen ETB, Fenton RA. Aquaporin-2 membrane targeting: still a conundrum. Am J Physiol. 2017; 312:F744–F747.

Olesen ETB, Moeller HB, Assentoft M, MacAulay N, Fenton RA. The vasopressin type 2 receptor and prostaglandin receptors EP2 and EP4 can increase aquaporin-2 plasma membrane targeting through a cAMP-independent pathway. Am J Physiol. 2016; 311:F935–F944.

Olesen ETB, Rutzler MR, Moeller HB, Praetorius HA, Fenton RA. Vasopressin-independent targeting of aquaporin-2 by selective E-prostanoid receptor agonists alleviates nephrogenic diabetes insipidus. Proc Natl Acad Sci. 2011; 108:12949–12954. [PubMed: 21768374]

Oliver JA. Nephrons and kidneys: A quantitative study of developmental and evolutionary mammalian renal architectonics. Harper and Row; New York: 1968.

Olives B, Neau P, Bailly P, Hediger MA, Rousselet G, Cartron J-P, Ripoche P. Cloning and functional expression of a urea transporter from human bone marrow cells. J Biol Chem. 1994; 269:31649–31652. [PubMed: 7989337]

Olives B, Mattei M-G, Huet M, Neau P, Martial S, Cartron J-P, Bailly P. Kidd blood group and urea transport function of human erythrocytes are carried by the same protein. J Biol Chem. 1995; 270:15607–15610. [PubMed: 7797558]

Pallone TL, Edwards A, Mattson DL. Renal medullary circulation. Compr Physiol. 2012; 2:97–140. [PubMed: 23728972]

Pallone TL, Turner MR, Edwards A, Jamison RL. Countercurrent exchange in the renal medulla. Am J Physiol. 2003; 284:R1153–R1175.

Pallone TL, Work J, Myers RL, Jamison RL. Transport of sodium and urea in outer medullary descending vasa recta. J Clin Invest. 1994; 93:212–222. [PubMed: 8282790]

Pannabecker TL. Structure and function of the thin limbs of the loops of Henle. In: Terjung RL, editorComprehensive physiology. Vol. 2. John Wiley and Sons, Bethesda; 2012. 2063–2086.

Pannabecker TL. Comparative physiology and architecture associated with the mammalian urine concentrating mechanism: role of inner medullary water and urea transport pathways in the rodent medulla. Am J Physiol. 2013; 304:R488–R503.

Pannabecker TL. Aquaporins in desert rodent physiology. Biol Bull. 2015; 229:120–128. [PubMed: 26338874]

Pannabecker TL, Dantzler WH. Three-dimensional lateral and vertical relationships of inner medullary loops of Henle and collecting ducts. Am J Physiol. 2004; 287:F767–F774.

Pannabecker TL, Dantzler WH. Three-dimensional architecture of inner medullary vasa recta. Am J Physiol. 2006; 290:F1355–F1366.

Pannabecker TL, Dantzler WH. Three-dimensional architecture of collecting ducts, loops of Henle, and blood vessels in the renal papilla. Am J Physiol. 2007; 293:F696–F704.

Pannabecker TL, Dantzler WH. Quantitative analysis of renal inner medullary structure. FASEB J. 2008; 22

Pannabecker TL, Dantzler WH, Layton HE, Layton AT. Role of three-dimensional architecture in the urine concentrating mechanism of the rat renal inner medulla. Am J Physiol. 2008a; 295:F1271–F1285.

Pannabecker TL, Henderson C, Dantzler WH. Quantitative analysis of functional reconstructions reveals lateral and axial zonation in the renal inner medulla. Am J Physiol. 2008b; 294:1306–1314.

Pannabecker TL, Layton A. Targeted delivery of solutes and oxygen in the renal medulla: role of microvessel architecture. Am J Physiol. 2014; 307:F649–F655.

Pannabecker TL, Rosen S. Outer stripe of the outer medulla in human and pig kidney is markedly reduced or absent compared to rat. J Am Soc Nephrol. 2017; 28:130. Abstract Supplement. [PubMed: 27151921]

Pearce D, Soundararajan R, Trimpert C, Kashlan OB, Deen PMT, Kohan DE. Collecting duct principal cell transport processes and their regulation. Clin J Am Soc Nephrol. 2015; 10:135–146. [PubMed: 24875192]

Perucca J, Bouby N, Valeix P, Bankir L. Sex difference in urine concentration across differing ages, sodium intake, and level of kidney disease. Am J Physiol. 2007; 292:R700–R705.

Potter EA, Stewart G, Smith CP. Urea flux across MDCK-mUT-A2 monolayers is acutely sensitive to AVP, cAMP, and $[Ca^{2+}]_i$. Am J Physiol. 2006; 291:F122–F128.

Peter KP. Untersuchungen uber bau und entwickelung der niere. Gustav Fischer; Jena: 1909.

Poulsen SB, Kim Y-H, Frokiaer J, Nielsen S, Christensen BM. Long-term vasopressin-V_2-receptor stimulation induces regulation of aquaporin 4 protein in renal inner medulla and cortex of Brattleboro rats. Nephrol Dial Transplant. 2013; 28:2058–2065. [PubMed: 23615760]

Promeneur D, Bankir L, Hu M-C, Trinh-Trang-Tan M-M. Renal tubular and vascular urea transporters: influence of antidiuretic hormone on messenger RNA expression in Brattleboro rats. J Am Soc Nephrol. 1998; 9:1359–1366. [PubMed: 9697657]

Qian X, Sands JM, Song X, Chen G. Modulation of kidney urea transporter UT-A3 activity by alpha2,6-sialylation. Pflugers Arch. 2016; 468:1161–1170. [PubMed: 26972907]

Ramkumar N, Stuart D, Calquin M, Quadri S, Wang S, van Hoek AN, Siragy HM, Ichihara A, Kohan DE. Nephron-specific deletion of the prorenin receptor causes a urine concentration defect. Am J Physiol. 2015; 309:F48–F56.

Ren H, Gu L, Andreasen A, Thomsen JS, Cao L, Christensen EI, Zhai XY. Spatial organization of the vascular bundle and the interbundle region: three-dimensional reconstruction at the inner stripe of the outer medulla in the mouse kidney. Am J Physiol. 2014; 306:F321–326.

Rieg T, Tang T, Uchida S, Hammond HK, Fenton RA, Vallon V. Adenylyl cyclase 6 enhances NKCC2 expression and mediates vasopressin-induced phosphorylation of NKCC2 and NCC. Am J Pathol. 2013; 182:96–106. [PubMed: 23123217]

Rollhauser H, Kriz W, Heinke W. Das gefass-system der rattenniere. Zeitschrift fur Zellforschung. 1964; 64:381–403.

Rutishauser J, Kopp P. Aquaporin-2 water channel mutation and nephrogenic diabetes insipidus: new variation on a theme. Eur J Endocrinol. 1999; 140:137–139. [PubMed: 10069656]

Sakuma Y, Nonoguchi H, Takayama M, Yang T, Terada Y, Inoue T, Nakayama Y, Kohda Y, Sasaki S, Tomita K. Differential effects of hyperosmolality on Na-K-ATPase and vasopressin-dependent cAMP generation in the medullary thick ascending limb and outer medullary collecting duct. Hypertens Res. 2005; 28:671–679. [PubMed: 16392772]

Sands JM, Blount MA. Genes and proteins of urea transporters. Subcell Biochem. 2014; 73:45–64. [PubMed: 25298338]

Sands JM, Knepper MA. Urea permeability of mammalian inner medullary collecting duct system and papillary surface epithelium. J Clin Invest. 1987; 79:138–147. [PubMed: 3793921]

Sands JM, Layton HE. Advances in understanding the urine-concentrating mechanism. Annu Rev Physiol. 2014; 76:387–409. [PubMed: 24245944]

Sands JM, Nonoguchi H, Knepper MA. Vasopressin effects on urea and H_20 transport in inner medullary collecting duct subsegments. Am J Physiol. 1987; 253:F823–F832. [PubMed: 3688238]

Satake M, Ikarashi N, Kagami M, Ogiue N, Toda T, Kobayashi Y, Ochiai W, Sugiyama K. Increases in the expression levels of aquaporin-2 and aquaporin-3 in the renal collecting tubules alleviate dehydration associated with polyuria in diabetes mellitus. Biol Pharm Bull. 2010; 12:1965–1970.

Saxen L. Organogenesis of the kidney. Cambridge University Press; Cambridge, UK: 1987.

Schmidt-Nielsen B. The renal concentrating mechanism in insects and mammals: a new hypothesis involving hydrostatic pressures. Am J Physiol. 1995; 268:R1087–R1100. [PubMed: 7539594]

Schwartz MM, Karnovsky MJ, Venkatachalam MA. Regional membrane specialization in the thin limbs of Henle loops as seen by freeze-fracture electron-microscopy. Kidney Int. 1979; 16:577–589. [PubMed: 548602]

Schwartz MM, Venkatachalam MA. Structural differences in thin limbs of Henle: physiological implications. Kidney Int. 1974; 6:193–208. [PubMed: 4427417]

Sever R, Glass CK. Signaling by nuclear receptors. Cold Spring Harb Perspect Biol. 2013; 5:a016709. [PubMed: 23457262]

Shayakul C, Steel A, Hediger MA. Molecular cloning and characterization of the vasopressin-regulated urea transporter of rat kidney collecting ducts. J Clin Invest. 1996; 98:2580–2587. [PubMed: 8958221]

Shayakul C, Knepper MA, Smith CP, DiGiovanni SR, Hediger MA. Segmental localization of urea transporter mRNAs in rat kidney. Am J Physiol. 1997; 272:F654–F660. [PubMed: 9176377]

Shayakul C, Smith CP, Mackenzie HS, Lee W-S, Brown D, Hediger MA. Long-term regulation of urea transporter expression by vasopressin in Brattleboro rats. Am J Physiol. 2000; 278:F620–F627.

Shayakul C, Tsukaguchi H, Berger UV, Hediger MA. Molecular characterization of a novel urea transporter from kidney inner medullary collecting ducts. Am J Physiol. 2001; 280:F487–F494.

Skorecki KL, Brown D, Ercolani L, Ausiello DA. Molecular mechanisms of vasopressin action in the kidney. Compr Physiol. 2011:1185–1218.

Smith CP, Lee W-S, Martial S, Knepper MA, You G, Sands JM, Hediger MA. Cloning and regulation of expression of the rat kidney urea transporter (rUT2). J Clin Invest. 1995; 96:1556–1563. [PubMed: 7657826]

Smith CP, Potter EA, Fenton RA, Stewart GS. Characterization of a human colonic cDNA encoding a structurally novel urea transporter, hUT-A6. Am J Physiol. 2004; 287:C1087–C1093.

Soodvilai S, Jia Z, Fongsupa S, Chatsudthipong V, Yang T. Liver X receptor agonists decrease ENaC-mediated sodium transport in collecting duct cells. Am J Physiol. 2012; 303:F1610–F1616.

Sonntag SR, Ziemans A, Wulfmeyer VC, Milatz S, Bleich M, Himmerkus N. Diuretic state affects ascending thin limb tight junctions. Am J Physiol. 2018; 314:F190–195.

Stephenson JL. Concentration of urine in a central core model of the renal counterflow system. Kidney Int. 1972; 2:85–94. [PubMed: 4671532]

Stewart GS, Fenton RA, Wang W, Kwon T-H, White SJ, Collins VM, Cooper G, Nielsen S, Smith CP. The basolateral expression of mUT-A3 in the mouse kidney. Am J Physiol. 2004; 286:F979–F987.

Stewart GS, King SL, Potter EA, Smith CP. Acute regulation of mUT-A3 urea transporter expressed in a MDCK cell line. Am J Physiol. 2007; 292:F1157–F1163.

Su W, Huang S-Z, Gao M, Kong X-M, Gustafsson J-Å, Xu S-J, Wang B, Zheng F, Chen L-H, Wang N-P, Guan Y-F, Zhang X-Y. Liver X receptor increases aquaporin 2 protein level via a posttranscriptional mechanism in renal collecting ducts. Am J Physiol. 2017; 312:F619–F628.

Tamura Y, Mori N, Xu B, Nakamura T, Yamakoshi S, Hirose T, Ito O, Totsune K, Takahashi K, Kohzuki M. Water deprivation increases (pro)renin receptor levels in the kidney and decreases plasma concentrations of soluble (pro)renin receptor. Tohoku J Exp Med. 2016; 239:185–192. [PubMed: 27350190]

Terris J, Ecelbarger CA, Marples D, Knepper MA, Nielsen S. Distribution of aquaporin-4 water channel expression within rat kidney. Am J Physiol. 1995; 269:F775–F785. [PubMed: 8594871]

Terris J, Ecelbarger CA, Nielsen S, Knepper MA. Long-term regulation of four renal aquaporins in rats. Am J Physiol. 1996; 271:F414–F422. [PubMed: 8770174]

Terris JM, Knepper MA, Wade JB. UT-A3: localization and characterization of an additional urea transporter isoform in the IMCD. Am J Physiol. 2001; 280:F325–F332.

Thomas SR. Inner medullary lactate production and accumulation: a vasa recta model. Am J Physiol. 2000; 279:F468–F481.

Thomas SR, Wexler AS. Inner medullary external osmotic driving force in a 3-D model of the renal concentrating mechanism. Am J Physiol. 1995; 269:F159–F171. [PubMed: 7653590]

Trimpert C, Wesche D, de Groot T, Pimentel Rodriguez MM, Wong V, van den Berg DTM, Cheval L, Ariza CA, Doucet A, Stagljar I, Deen PMT. NDFIP allows NEDD4/NEDD4L- induced AQP2 ubiquitination and degradation. PLoS ONE. 2017; 12(9):e0183774. [PubMed: 28931009]

Trinh-Trang-Tan M-M, Lasbennes F, Gane P, Roudier N, Ripoche P, Cartron J-P, Bailly P. UT-B1 proteins in rat: tissue distribution and regulation by antidiuretic hormone in kidney. Am J Physiol. 2002; 283:F912–F922.

Uchida S, Sohara E, Rai T, Ikawa M, Okabe M, Sasaki S. Impaired urea accumulation in the inner medulla of mice lacking the urea transporter UT-A2. Mol Cell Biol. 2005; 25:7357–7363. [PubMed: 16055743]

Urity VB, Issaian T, Braun EJ, Dantzler WH, Pannabecker TL. Architecture of kangaroo rat inner medulla: segmentation of descending thin limb of Henle's loop. Am J Physiol. 2012; 302:R720–R726.

van Hoek AN, Bouley R, Lu Y, Silberstein C, Brown D, Wax MB, Patil RV. Vasopressin-induced differential stimulation of AQP4 splice variants regulates the in-membrane assembly of orthogonal arrays. Am J Physiol. 2009; 296:F1396–F1404.

Wade JB, Lee AJ, Liu J, Ecelbarger CA, Mitchell C, Bradford AD, Terris J, Kim G-H, Knepper MA. UT-A2: a 55 kDa urea transporter in thin descending limb whose abundance is regulated by vasopressin. Am J Physiol. 2000; 278:F52–F62.

Wang F, Lu X, Peng K, Fang H, Zhou L, Su J, Nau A, Yang KT, Ichihara A, Lu A, Zhou S-F, Yang T. Antidiuretic action of collecting duct (pro)renin receptor downstream of vasopressin and PGE_2 receptor EP_4. J Am Soc Nephrol. 2016a; 27:3022–3034. [PubMed: 27000064]

Wang J, Wang XH, Wang H, Chen L, Klein JD, Sands JM. Urea transporter B and microRNA-200c differ in kidney outer versus inner medulla following dehydration. Am J Med Sci. 2016b; 352:296–301. [PubMed: 27650235]

Wang X, Thomas SR, Wexler AS. Outer medullary anatomy and the urine concentrating mechanism. Am J Physiol. 1998; 274:F413–F424. [PubMed: 9486237]

Wang Y, Klein JD, Blount MA, Martin CF, Kent KJ, Pech V, Wall SM, Sands JM. Epac regulates UT-A1 to increase urea transport in inner medullary collecting ducts. J Am Soc Nephrol. 2009; 20:2018–2024. [PubMed: 19661162]

Wang Y, Klein JD, Liedtke CM, Sands JM. Protein kinase C regulates urea permeability in the rat inner medullary collecting duct. Am J Physiol. 2010; 299:F1401–F1406.

Wang Y, Klein JD, Froehlich O, Sands JM. Role of protein kinase C- in hypertonicity-stimulated urea permeability in mouse inner medullary collecting ducts. Am J Physiol. 2013; 304:F233–F238.

Wei G, Rosen S, Dantzler WH, Pannabecker TL. Architecture of the human renal inner medulla and functional implications. Am J Physiol. 2015; 309:F627–F637.

Westrick KY, Serack BJ, Dantzler WH, Pannabecker TL. Axial compartmentation of descending and ascending thin limbs of Henle's loops. Am J Physiol. 2013; 304:F308–F316.

Wu Q, Moeller HB, Stevens DA, Sanchez-Hodge R, Childers G, Kortenoeven MLA, Cheng L, Rosenbaek LL, Rubel C, Patterson C, Pisitkun T, Schisler JC, Fenton RA. CHIP regulates aquaporin-2 quality control and body water homeostasis. J Am Soc Nephrol. 2017; 29:936–948. [PubMed: 29242247]

Xu Y, Olives B, Bailly P, Fischer E, Ripoche P, Ronco P, Cartron J-P, Rondeau E. Endothelial cells of the kidney vasa recta express the urea transporter HUT11. Kidney Int. 1997; 51:138–146. [PubMed: 8995727]

Yamamoto K, Wilson DR, Baumal R. Blood supply and drainage of the outer medulla of the rat kidney: scanning electron microscopy of microvascular casts. Anat Rec. 1984; 210:273–277. [PubMed: 6507893]

Yang B, Bankir L. Urea and urine concentrating ability: new insights from studies in mice. Am J Physiol. 2005; 288:F881–F896.

Yang B, Bankir L, Gillespie A, Epstein CJ, Verkman AS. Urea-selective concentrating defect in transgenic mice lacking urea transporter UT-B. J Biol Chem. 2002; 277:10633–10637. [PubMed: 11792714]

Yao L, Huang D-Y, Pfaff IL, Nie X, Leitges M, Vallon V. Evidence for a role of protein kinase C- in urine concentration. Am J Physiol. 2004; 287:F299–F304.

You G, Smith CP, Kanai Y, Lee W-S, Stelzner M, Hediger MA. Cloning and characterization of the vasopressin-regulated urea transporter. Nature. 1993; 365:844–847. [PubMed: 8413669]

Yuan J, Pannabecker TL. Architecture of inner medullary descending and ascending vasa recta: pathways for countercurrent exchange. Am J Physiol. 2010; 299:F265–F272.

Zhai X-Y, Thomsen JS, Birn H, Kristoffersen IB, Andreasen A, Christensen EI. Three-dimensional reconstruction of the mouse nephron. J Am Soc Nephrol. 2006; 17:77–88. [PubMed: 16319188]

Zhai X-Y, Fenton RA, Andreasen A, Thomsen JS, Christensen EI. Aquaporin-1 is not expressed in descending thin limbs of short-loop nephrons. J Am Soc Nephrol. 2007; 18:2937–2944. [PubMed: 17942963]

Zhang X-Y, Wang B, Guan Y-F. Nuclear receptor regulation of aquaporin-2 in the kidney. Int J Mol Sci. 2016; 17:1105.

Zhang Y, Peti-Peterdi J, Muller CE, Carlson NG, Baqi Y, Strasburg DL, Heiney KM, Villanueva K, Kohan DE, Kishore BK. $P2Y_{12}$ receptor localizes in the renal collecting duct and its blockade augments arginine vasopressin action and alleviates nephrogenic diabetes insipidus. J Am Soc Nephrol. 2015; 26:2978–2987. [PubMed: 25855780]

Zhao H, Wiederkehr MR, Fan L, Collazo RL, Crowder LA, Moe OW. Acute inhibition of Na/H exchanger NHE-3 by cAMP. Role of protein kinase A and NHE-3 phosphoserines 552 and 605. J Biol Chem. 1999; 274:3978–3987. [PubMed: 9933588]

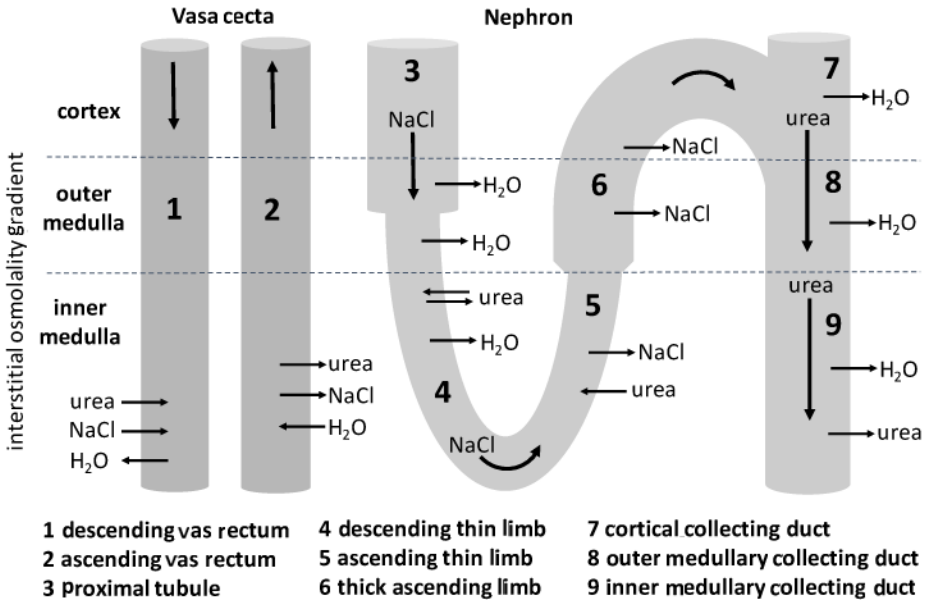

Fig. 1.

The direction of urea, NaCl, and H_2O movement in the vasa recta and long-looped nephron according to countercurrent multiplication and the passive mechanism. See text for details.

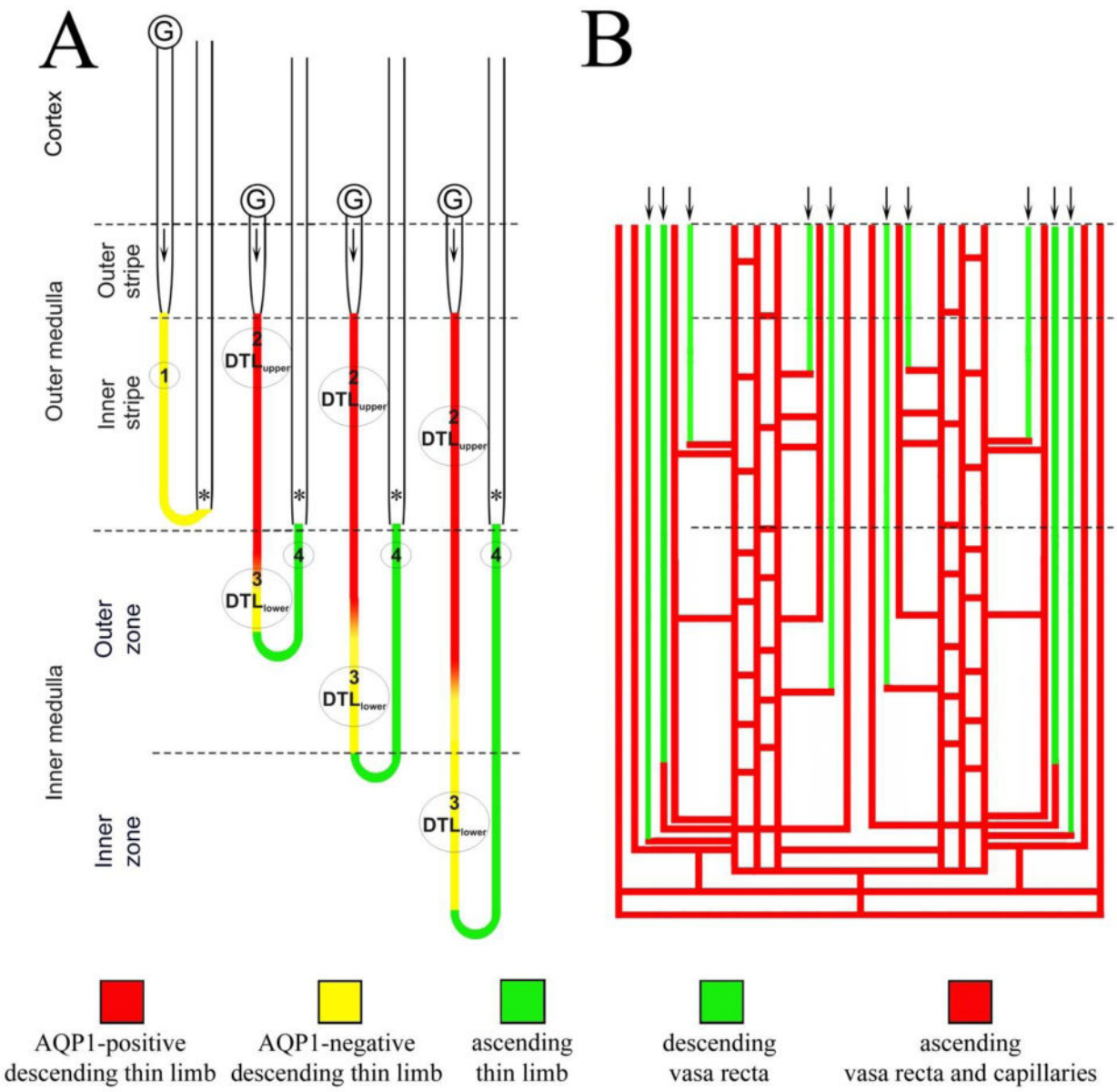

Fig. 2.

Schematic diagram illustrating the rodent renal medullary nephron segments and blood vessels. A: Four types of thin limbs of Henle's loops exist in the rodent kidney and include the type 1 (short-looped descending thin limb), type 2 (AQP1-positive long-looped descending thin limb or DTL_{upper}), type 3 (AQP1-negative long-looped descending thin limb or DTL_{lower}) and type 4 (ascending thin limb). Arrow in the proximal straight segment shows flow direction; asterisk identifies thick ascending limb. B: The renal blood vessels consist of the unbranched descending and ascending vasa recta. Descending vasa recta connect to capillaries that join a network of branching AVR at any level of the medulla. The capillary networks return plasma to the cortex either directly or by way of the ascending vasa recta.

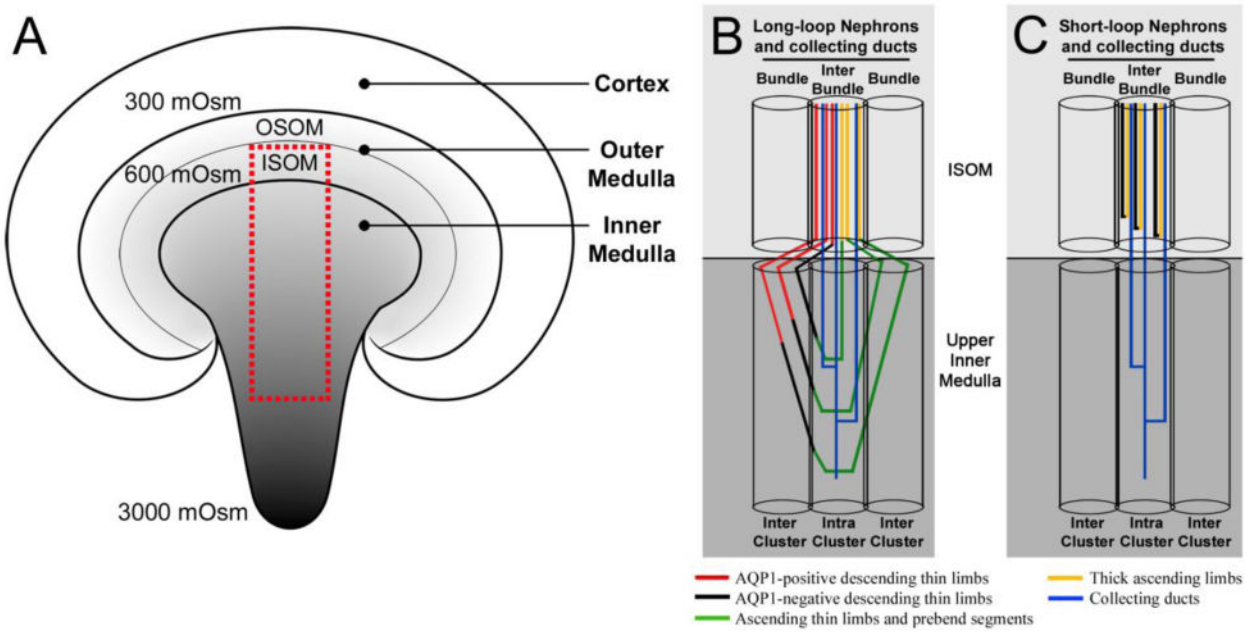

Fig. 3.

Diagrammatic coronal section of the rodent kidney and medullary nephron and collecting duct architecture. A: The corticomedullary osmotic gradient increases from the cortex to the tip of the inner medulla (reaching a maximum of 3000 mOsmol kg^{-1} H_20 in the rat). OSOM, outer stripe of the outer medulla; ISOM, inner stripe of the outer medulla. The red box represents the area occupied by nephrons and collecting ducts shown in B and C. The medullary architecture of long-loop nephrons (B) and short-loop nephrons (C) is depicted in schematic diagrams alongside collecting duct (CD) clusters. The ISOM consists of two lateral regions (bundle and interbundle) and the upper inner medulla consists of two lateral regions (intercluster and intracluster). Modified from Wei et al. 2015, with permission.

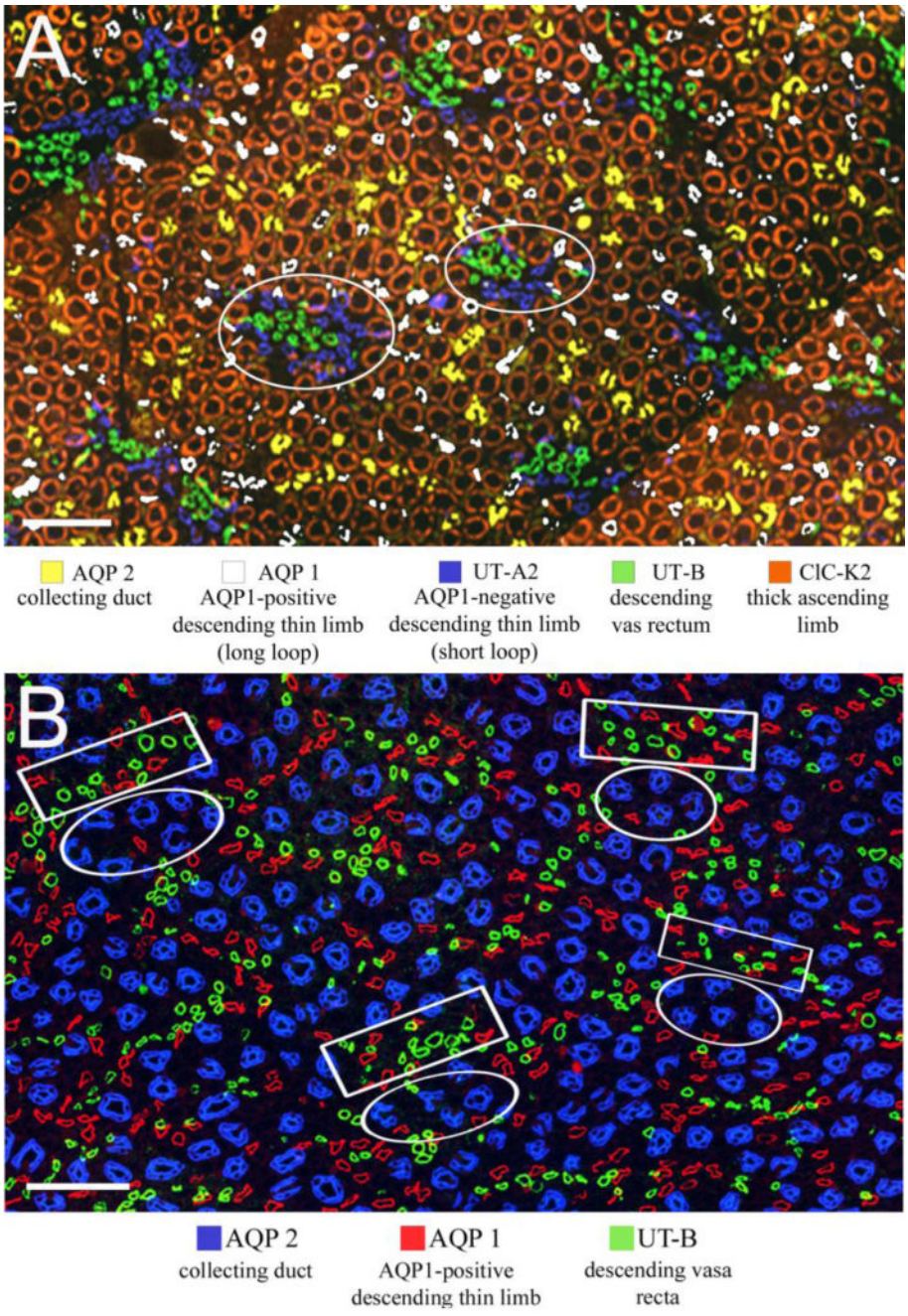

Fig. 4.

Immunolocalization of tubules and vessels in the Munich-Wistar medulla. A: Inner stripe of the outer medulla. Bundle regions (two are circled) consist of DVR, unbranched AVR (not shown) and short loop DTLs. Interbundle regions consist of long-loop DTLs, thick ascending limbs, CDs and networks of branching AVR (AVR are not shown). B: Inner medulla (approximately 900 μm below the outer medulla). Intracluster regions (circles) consist of CDs, descending and ascending thin limbs and networks of branching AVR (the latter three are not shown). The intercluster regions (boxes) consist of descending and

ascending thin limbs, DVR and AVR (ATLs and AVR are not shown). Scale bars: 100 μm. Modified from Pannabecker 2013, with permission.

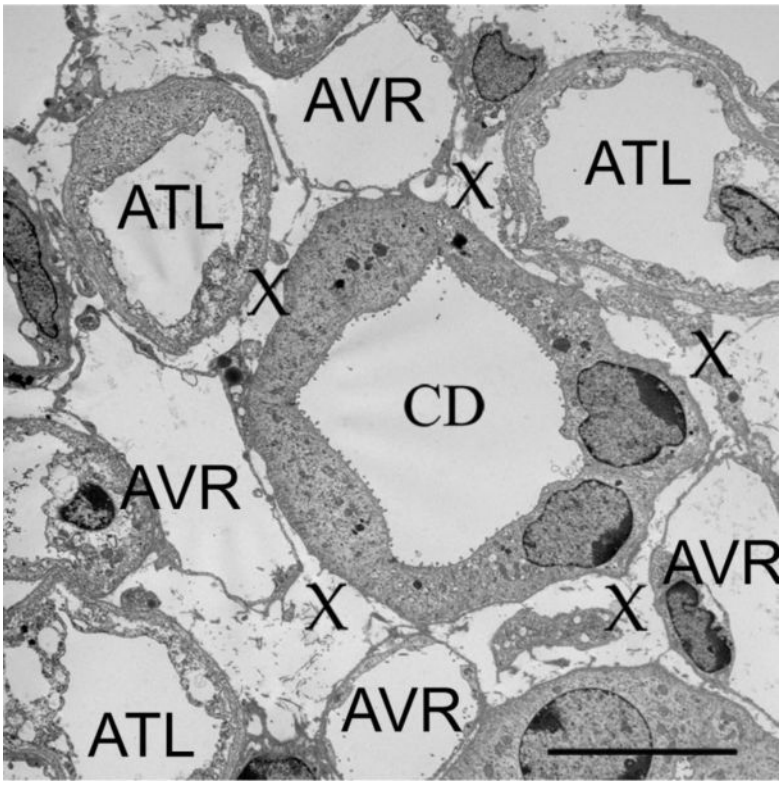

Fig. 5.

Ultrastructure of interstitial nodal spaces in a transverse ultrathin section from kangaroo rat inner medulla. Interstitial nodal spaces are marked with an X. AVR, fenestrated ascending vasa recta; ATL, ascending thin limb; CD, collecting duct. Section is from midway between the outer medullary-inner medullary boundary and papilla tip. Scale bar, 10 μm. Reproduced from Issaian et al. 2012, with permission.

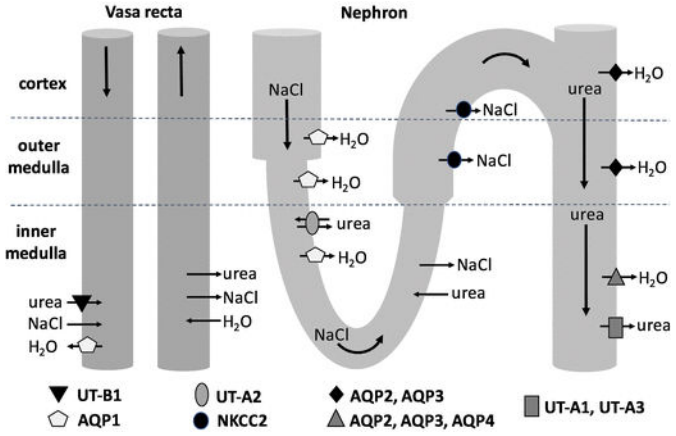

Fig. 6.

Location of major transporters involved in the urine-concentrating mechanism in the vasa recta and long-looped nephron.

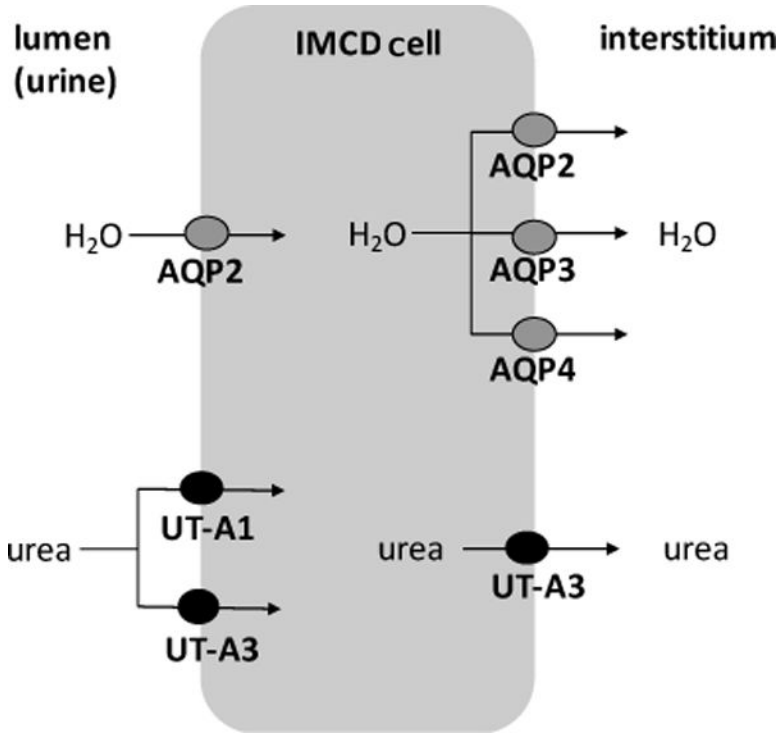

Fig. 7.

Apical (lumen) and basolateral (interstitium) localization of urea transporters and aquaporins in the inner medullary collecting duct (IMCD) cell.

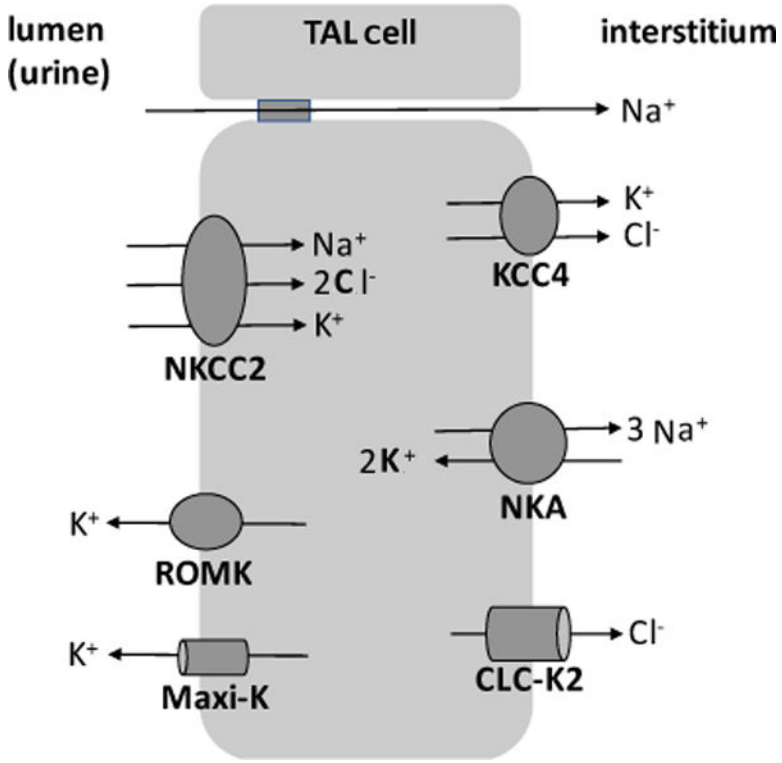

Fig. 8.

Major transporters involved in urine concentration in the thick ascending limb (TAL) cell. Na^+-K^+-2 Cl^- cotransporter 2 (NKCC2); renal outer medullary K^+ channel (ROMK); Ca^{++}-activated maxi K^+ channel (Maxi-K^+); K^+-Cl^- cotransporter 4 (KCC4); Na^+-K^+-ATPase (NKA); chloride channel (CLC-K2). See text for details.